J. Fluid Mech. (1989), *vol.* 204, *pp.* 295–324
Printed in Great Britain

A new equation for calculating wave loads on offshore structures

By R. C. T. RAINEY
WS Atkins Engineering Sciences, Woodcote Grove, Epsom, Surrey KT18 5BW, UK

(Received 30 March 1988 and in revised form 10 October 1988)

This paper derives an equation for the potential-flow wave loading on a lattice-type offshore structure moving partially immersed in waves. It is for the limiting case of small lattice-member diameter, and deals entirely in member-centreline fluid properties, so that it can be applied computationally by a simple 'stick model' computer program. This field is currently served by a simple two-term semi-empirical formula 'Morison's equation': the new equation is effectively a replacement for the Morison inertial term, allowing the Morison drag term (or some refinement of it) to describe exclusively the effects of vorticity, which can in principle be calculated to greater accuracy when isolated in this way.

The new equation calculates the potential-flow wave load accurate to second order in wave height, which is a great improvement on 'Morison's equation': such results can currently only be sought by very much more complicated and computationally intensive methods, of currently uncertain repeatability. Moreover the third-order error is localized at the free-surface intersection, so the equation remains attractive for fully nonlinear problems involving intermittent immersion of lattice members, which are currently beyond even the most sophisticated of these computationally intensive methods. It is shown that the primary reason for this large contrast in computational efficiency is that the loads are derived from energy considerations rather than direct integration of surface pressures, which requires a lower level of flow detail for a given level of load-calculation accuracy.

These improvements must of course be seen against the current levels of uncertainty over the calculation of vorticity-induced loads, which in many applications completely dwarf inaccuracies in potential-flow load calculation. The conditions are accordingly established under which the improvements are comparable to the total wave load predicted by the Morison drag and inertia terms in combination. They are that the lattice member diameter is greater than its length/10, or the relative fluid motion/5, or the structure's motion radius/20, or the wavelength/30: if any one of these conditions is satisfied, the new equation is worthwhile even when used in combination with simple vorticity-induced load calculations from a Morison drag term.

1. Introduction

There are at present three basic approaches to calculating wave loads on lattice-type offshore structures (i.e. frameworks built of cylinders of arbitrary cross-section and orientation). The first is to assume that the flow around each section of the lattice is as it would be if that section were immersed in a uniform cross-flow with acceleration and velocity equalling those (normal to the member) in the undisturbed incident wave at that point. The wave load in such uniform cross-flow is known from

experiments in a U-tube oscillating water column apparatus, and can be expressed empirically by 'Morison's equation' as an inertial term proportional to the acceleration, plus a drag term proportional to the velocity squared. Thus the wave load on any lattice structure can be predicted by 'Morison's equation', with very little computational effort.

The second approach is not restricted to lattice structures but can be applied to them. It is to assume that the flow is irrotational (i.e. ignore the boundary layers and all the wakes produced by flow separation) and describe the flow as a power series in wave height by Stokes' expansion, so as to give first-order wave loads proportional to wave height, second-order wave loads proportional to (wave height)^2, and so on. For calculating the first-order loads, much the most widely used computational procedure is to distribute over the structure's surface a large number of wave-radiating hydrodynamic point sources and/or dipoles. The mathematical expressions for the flow from an individual source and dipole is given in Wehausen & Laitone (1960) following the expressions of Lamb (1932, §§242–245) which were first studied in detail for this application by John (1950). Their complexity, and the inherent abstraction of the procedure for the simultaneous adjustment of all the source/dipole strengths to solve any particular problem, means that computer programs using this method are prone to a variety of modest systematic errors, and also need large computing resources. This is particularly true when they are applied to lattices; Eatock-Taylor & Jefferys (1986) report answers (for non-trivial parameters like added mass) typically scattered over a range 1.5:1 from a number of nominally identical programs from different authors, and Korsmeyer *et al.* (1988) give results and computing times with a very highly optimized program. These latter show that for first-order calculations each lattice member needs at least fifty panels (i.e. sources and dipoles), and that a modest ten-member lattice (or thirty members taking computational advantage of two planes of symmetry) will require 10 h computing per wave case on a typical medium-sized (0.5 Mflop) computer. For more complex lattices, the computing time rises as the square of the number of panels (itself an advance; with earlier programs it rises eventually as the cube).

The third approach is again not limited to lattice structures, and again assumes irrotational flow. It is to simulate the fully nonlinear motion of the water surface by means of primitive hydrodynamic sources, dipoles or vortices distributed over this moving free surface as well as over the instantaneous wetted surface of the structure. This type of procedure was originally developed for studying breaking waves (Longuet-Higgins & Cokelet 1976); it is completely general and can in principle handle highly nonlinear effects such as the intermittent immersion of a lattice member, which is inherently beyond Stokes' expansion. However, the approach poses deep problems of numerical stability and requires much larger computing resources than the second approach above – at the present time it has only been applied to single fixed horizontal cylinders parallel to the wave crests (Vinje & Brevig 1981) and to single circular vertical cylinders (Isaacson 1982).

This paper is concerned with improvements to the first ('Morison's equation') approach. It was argued by Lighthill (1979, 1986*b*) that the hydrodynamic loading on a lattice-type offshore structure, where the member diameters are small compared with the wavelength, should be analysed as the sum of the loading due to the potential flow alone, and the loading due to the remaining vorticity-induced flow alone. He pointed out that although in uniform cross-flow (i.e. the conditions in a U-tube apparatus) the Morison inertia term did indeed precisely correspond to the potential-flow load, *it did not do so in the non-uniform flow conditions of waves*. In

particular, he showed (Lighthill 1979) that the velocity gradients resulting from flow non-uniformities produce a contribution to the potential-flow load on a fixed vertical circular cylinder which does not fall (as a proportion of that load) as the cylinder diameter is reduced. At first sight this might appear to be explained by the contribution made by velocity gradients to water particle acceleration (e.g. in the steady but accelerating flow in a narrowing pipe). In particular, it was shown by Isaacson (1979, equation 28) that for a fixed horizontal circular cylinder (parallel to the wave crests) the Morison inertia term correctly describes the potential-flow loads, if it is based on full particle accelerations. Unfortunately this explanation is not a general one: Lighthill's vertical-cylinder result cannot be reproduced by that means.

In terms of Stokes' expansion, these potential-flow loads from velocity gradients are of second order in wave height, like the Morison drag term (the Morison inertia term being first order in wave height). Rather than use that term to describe them empirically, Lighthill's proposal is that the Morison inertia term be replaced by the potential-flow load calculated accurately to second order in wave height. In this way the Morison drag term is left exclusively for describing the vorticity-induced load, and may in its turn one day be refined, since vorticity-induced load can in principle be accurately calculated using a modified version of the well-known formula for the momentum of a vortex flow (see e.g. Batchelor 1967, equation 7.2.5). Lighthill has in mind second-order potential-flow calculations carried out, as for his vertical cylinder, by finding the limiting form of the Stokes' expansion results as the cylinder diameter is reduced. Thus his proposed replacement for Morison's inertia term is unified with the second approach described above, by giving answers in agreement with it if the lattice member diameters are sufficiently small.

The problem addressed by this paper is that of obtaining an explicit general equation for these limiting forms, so that the result can be applied computationally in the same way as Morison's equation, using a 'stick model' of the lattice structure rather than the very much more complicated 'panel model' required by the second approach above. In fact the equation derived requires about 0.1 s per timestep per lattice member on a 0.5 Mflop computer, so that it is practicable to analyse the most complex structures with thousands of cylindrical elements, which from the above figures are commercially impractical, even to first order in wave height, even with the fastest panel programs. Being a simple explicit equation, it is also not prone to the various systematic errors of panel programs referred to above, which in most cases more than compensates for its additional approximation that the lattice member diameters are small.

The argument used to derive the new equation begins with a review in §2 below of the general features of the potential flow around a cylinder in the most general moving finite-length partially immersed case, as its diameter is reduced relative to the wavelength (and any other lengths defining the problem), following the procedure in Lighthill (1979). It is explained that the source of Lighthill's second-order vertical-cylinder load is not only the direct effects of the velocity gradient, but also the small component of the diffracted flow parallel to the cylinder axis, which is why his result is different from Isaacson's (1979) one (Isaacson's horizontal cylinder is a two-dimensional problem with zero axial flow). Moreover, it is shown that the local flow at a cylinder end, or at a free-surface intersection (except in Lighthill's vertical-cylinder example, which is atypically simple), also produces a second-order wave load, which is precisely comparable in that it too does not fall (as a proportion of the total potential-flow load) as the cylinder diameter is reduced.

At first sight, therefore, the general problem of second-order potential-flow loads

on lattices appears prohibitively complicated. It is next shown in §3, however, that in two simple classical examples – a cylinder translating in still water and a small body fixed in converging flow – all this complexity is avoided by using (respectively) a momentum and an energy argument to deduce the fluid load. This suggests that in general *less flow details are required to calculate fluid loads by either of these means, than by direct integration of surface pressures.* It motivates the energy argument of the remainder of the paper, and explains why the final result is so simple, using as it does only a simple 'stick model' to characterize the flow, and omitting all the flow details just cited above as the apparent 'cause' of second-order wave loads. It also means that the contrast between such a 'stick model' and the kind of beautiful detailed lattice-structure 'panel model' shown by Korsmeyer *et al.* (1988) is not as stark as it may seem: the latter has of necessity to be more detailed, because it is used for surface pressure integration, which is evidently a much less efficient method of determining wave loads.

The crucial approximation of this paper, which enables a classical energy argument to be used, is that *the position of the wave surface is unaffected by the presence of the structure.* This removes the free-surface degrees of freedom from the problem, so that it can be tackled by classical energy arguments (i.e. Kelvin & Tait's argument rigorously proved by Lamb (1932, §136); this paper has no relation to recent attempts (e.g. Miloh 1984) at using energy arguments when the free-surface freedoms are retained). This approach is much less restrictive than the traditional Froude–Krilov approximation, which is that not only the surface position of the waves, *but also the pressure in them*, are unaffected by the presence of the structure. Indeed, it is shown in §4 that for our limiting case of small-diameter cylinders, the effects of our 'wavy lid' approximation are localized at the intersections of lattice members with the free surface – elsewhere the effect is nil. In terms of Stokes' expansion, it is in fact shown that the error introduced by the approximation is of third order in wave height, which meets the original specification for second-order accuracy laid down as described above by Lighthill (1979). Equally important, however, is the fact that the error is localized – this means that the approximation remains attractive for the many practical problems of very large nonlinear structural and fluid motions, where the Stokes' expansion procedure of a perturbation analysis about the mean position of the free surface (and, for a moving structure, the mean structural position) is clearly inappropriate. An interesting example is the case of a breaking wave, in which it has been shown by Peregrine, Cokelet & McIver (1980; further details in New, McIver & Peregrine 1985) that the velocity gradients produce accelerations up to $5g$ behind the vertical wave face, very forcibly focusing attention on the effects of velocity gradients described above. Peregrine's work is presently the fullest development of the third analytical approach described above; the results of this paper are therefore of interest through their link with that approach as well as through their link with Stokes' expansion methods.

The energy argument itself is completed in §§5 and 6, with the algebra kept manageable by means of a special notation summarized for convenience in Appendix A. It is first shown, in §5, that the fluid kinetic energy around an arbitrary lattice can be described by a simple stick model formula, the contributions from the various flow details cited above vanishing in our thin-cylinder limit, despite the fact that their contributions to the integral of surface pressure do *not* vanish, as stressed above. It is then shown in §6 that the Lagrange coordinates of the classical energy argument can be eliminated because of the quadratic form of the energy expression, so as to give an equation of motion in the simple vector form required for general application.

(The quadratic form is incidentally not dependent on the thin-cylinder limiting process, so the equation of motion is generally applicable to arbitrarily shaped bodies for which the fluid kinetic energy can be obtained by other means. An offshore-structure example is large seabed template structures during their installation by crane from the surface, in which they interact hydrodynamically with the seabed. The fluid kinetic energy can here be estimated, or if necessary computed with a standard finite-element computer program, for various seabed separation distances and attitudes, and the equation can then be used to find the motions of the template structure.)

The paper concludes with a study in §7 of the circumstances under which the new equation is a worthwhile improvement over Morison's equation' at present, i.e. even when combined with simple calculations of vorticity-induced load using the Morison drag term. To do this, the improvement is isolated by subtracting the load predicted by the Morison inertia term from the potential-flow loads predicted by the new equation, and the result is compared with the *total* load predicted by Morison's equation. The improvements are categorized according to the surface-pressure 'causes' elucidated in §2, viz: (*a*) steady-flow end effects, (*b*) unsteady-flow end effects, (*c*) longitudinal diffracted/radiated flow effects, (*d*) direct effects of incident velocity gradients; and in each case the criterion for a worthwhile improvement is derived in terms of the relevant non-dimensional parameter, which turns out to be the ratio of the cylinder diameter to (respectively) the cylinder length, the wave height, the radius of curvature of the structure's motion, and the wavelength. Section 7 also affords the opportunity of comparing the results of the new equation with the other relevant published results, all of which are special cases derived by other means. In all cases the new equation agrees as it should, after rectifying any errors in the other arguments used.

2. General features of the potential flow around a thin cylinder in waves

In this first Section the aim is to establish the general features of the potential flow around a thin finite-length cylinder of arbitrary cross-section moving in waves, for the general case of the cylinder at an arbitrary angle to the vertical, with one end out of the water and one in. By 'thin' we mean the limiting case of a cylinder whose radius b is reduced while the wavenumber $k(=2\pi/\text{wavelength})$ and the cylinder length (and water depth) are held constant, just as in Stokes' expansion we consider the limiting case of waves whose amplitude a is reduced in the same circumstances. In Stokes' expansion dimensioned quantities (i.e. pressures, velocities, etc.) are described as being of nth order in ka, meaning that if they are expressed as a function $f(ka)$, then $f(ka)/(ka)^n$ tends to a finite non-zero limit (with the original dimensions, i.e. pressure, velocity, etc.) as ka tends to zero. In exactly the same way, we shall describe dimensioned quantities as being of nth order in kb, with the precisely analogous meaning that if they are expressed as a function $f(kb)$ then $f(kb)/(kb)^n$ tends to a finite non-zero limit as kb tends to zero. Where necessary, we shall talk of ka-order and kb-order, rather than plain order, to avoid ambiguity. As a final refinement, we do not wish to exclude the case of a deeply immersed cylinder moving in the absence of incident waves, owing to some external excitation, in which situation the wavelength may be essentially irrelevant, and the radius to the instantaneous centre of rotation may have been introduced as another length in the problem. We shall therefore write $k'b$ for kb, and $k'a'$ for ka, to indicate that the limiting process makes (respectively) the cylinder radius, and all fluid motions

around the cylinder, small compared with *all* other lengths in the problem (wavelength, cylinder length, water depth, and radius to the instantaneous centre of rotation).

When a cylinder cuts the free water surface there is in fact a problem in considering the small-$k'b$ limit in isolation, because if a is held constant the pressure variations around the cylinder do not reduce to zero as b is reduced (the 'dynamic head' pressure gain at a stagnation point being independent of b), implying an ever-steeper slope of the free surface, so that the potential flow will become ever more badly behaved. Rather, therefore, we must for each b first consider the well-behaved limiting case of small a, in other words apply the two limiting procedures in the order:

$$\lim_{k'b\to 0}\left\{\lim_{k'a'\to 0}(\,)\right\}, \tag{2.1}$$

thereby effectively restricting our attention to the question of the $k'b$-order of quantities of given $k'a'$-order. The aim of this Section is accordingly limited to establishing the $k'b$-order of the various constituents of the first-$k'a'$-order flow around a thin cylinder, together with certain features of the second-$k'a'$-order wave loads, in the general case defined above.

It is convenient to begin by considering the special case of the first-$k'a'$-order flow from deep-water waves around a cylinder which is (i) fixed, (ii) vertical, (iii) circular and (iv) infinite in length. This classical problem was solved for all cylinder diameters by Havelock (1940, equation 17), and is a standard starting point in the offshore-structure literature, having been extended there to water of finite depth (MacCamy & Fuchs 1954) and more recently many attempts having been made to extend it to second $k'a'$-order. Our interest is restricted to the limiting case of small cylinder diameter, and moreover to the flow in the region close to the cylinder; for these purposes the Havelock expressions reduce to a simple form which can be derived directly, and much more simply, by an argument due to Lighthill (1979). The argument is based on the expansion of the fluid velocity v_i in the undisturbed incident wave as a Taylor series (see e.g. Batchelor 1967, equation 2.9.18) based its value $(v_i)_0$ and gradients at a fixed point, and position x_i relative to that point:

$$v_i = (v_i)_0 + x_j\frac{\partial v_i}{\partial x_j} + \tfrac{1}{2}x_j x_k\frac{\partial^2 v_i}{\partial x_i\,\partial x_k} + \ldots. \tag{2.2}$$

Applying this to the special case of a plane perpendicular to the cylinder (rather than three-dimensional space), over which the incident-wave velocity only varies with position downwave from the cylinder, gives (Lighthill 1979, equations 36–40) the first ka-order velocity potential of the incident wave ϕ_{I} in the form:

$$\phi_{\mathrm{I}} = (\phi_{\mathrm{I}})_0 + vr\cos\theta + \tfrac{1}{4}sr^2(1+\cos 2\theta) + \ldots, \tag{2.3}$$

where r and θ are polar coordinates about the cylinder axis ($\theta = 0$ being the propagation direction of the incident wave). $(\phi_{\mathrm{I}})_0$ is the value of ϕ_{I} on the axis, v is the component of the potential gradient $\nabla\phi$ on the axis in the direction $\theta = 0$, and s is the gradient of v on the axis in that direction: all three are functions of vertical position. We see that $vr\cos\theta$ is the potential derived from the incident velocity $(v_i)_0$ in (2.2), and $s(r\cos\theta)^2 = \frac{1}{2}sr^2(1+\cos 2\theta)$ is the potential derived from the incident velocity gradient $\partial v_i/\partial x_j$ in (2.2).

Lighthill then evaluated the first-$k'a'$-order diffracted potential ϕ_{D} as a series of circular harmonics (see e.g. Batchelor 1967, equation 2.10.5) which give the

necessary zero normal flow on the (circular) cylinder surface in combination with the corresponding terms of (2.3). This gives an expression beginning with the cylinder's response to the incident velocity, and then its response to the incident velocity gradient, and so on, thus:

$$\phi_{\mathrm{D}} = v\frac{b^2}{r}\cos\theta + \tfrac{1}{4}sb^2\left(-2\log_{\mathrm{e}} r + \frac{b^2}{r^2}\cos 2\theta\right) + \ldots . \tag{2.4}$$

The flow description is again three-dimensional because vertical variations are contained in v and s; at first sight that is problematical because circular harmonics only satisfy Laplace's equation if such vertical variations are eliminated. However, (2.4) (and indeed (2.3)) is only intended to represent the flow near the cylinder (i.e. for small kr); in this region Lighthill points out (as earlier in Lighthill 1960) that the higher $k'b$-order of the velocity gradient in the longitudinal direction along the cylinder axis, compared with the transverse direction perpendicular to it, enables circular harmonics to be used for our limiting case of small $k'b$. For independent confirmation of the whole argument, (2.3) and (2.4) may be seen to coincide with Havelock's expression (1940, equation 17) when both kr and $k'b$ are small.

Lighthill's method extends easily to the case of a cylinder of arbitrary cross-section moving in response to finite-depth waves at an arbitrary angle to the vertical, because we can in all cases expand ϕ_{I} in a cylindrical Taylor series like (2.3), this time about the mean position of the cylinder axis. Likewise we can always choose combinations of circular harmonics like (2.4) to satisfy the cylinder boundary condition; this time they represent the diffracted-plus-radiated potential. For our present purposes all we seek to establish is the $k'b$-order of the various constituents of the first $k'a'$-order diffracted-plus-radiated velocity field near the cylinder, which are readily deduced from linear wave theory (according to which v and s are proportional to $k\phi$ and kv, and their vertical gradients to kv and ks) and are shown in the first two columns of table 1. It is also simple to enter in table 1 the flow properties around a submerged cylinder end. The flow here is qualitatively similar to the flow around a sphere: the velocity is of the same $k'b$-order as that in the incident wave, and since the distances involved are of order $k'b$, the associated velocity potential and velocity gradient will be of order $k'b$ and $(k'b)^{-1}$ respectively, as shown.

A greater problem arises at the free surface. The potential of (2.4) conveniently satisfies the well-known first-$k'a'$-order free-surface boundary condition (Lighthill 1979, equation 12) holding at the still-water position, viz:

$$\frac{\partial^2\phi}{\partial t^2} + g\frac{\partial\phi}{\partial z} = 0 \tag{2.5}$$

(where t is time, z position measured vertically upwards, and g is the gravitational acceleration) because both v and s have the same type of t and z dependence as ϕ_{I}. In general, however, this is not so; a simple example being the radiated potential caused by transverse motion of a vertical cylinder, which clearly has a quite different type of z dependence from ϕ_{I}. Another example is a fixed cylinder inclined at an angle of 45° to the vertical; here the large (zeroth-$k'b$-order) transverse diffracted velocities shown in table 1 column 1 will have components normal to the water surface, which means that the diffracted potential analogous to (2.4) cannot satisfy (2.5) because the second term in (2.5) will be of zeroth $k'b$-order, but the first term in (2.5) will be of first $k'b$-order (like ϕ_{D}).

We have therefore to allow for some special additional effect at the intersection of

	Around main length of cylinder			Around an intersection with the free surface	
	Response to incident velocity; result of motion	Response to incident velocity gradient	Around a submerged end	Correction to give zero diffracted/radiated velocity normal to free surface	Further correction to satisfy free surface boundary condition
Longitudinal velocity (i.e. velocity along cylinder axis)	$k'b$	$(k'b)^2$	1	1	$k'b$
Transverse velocity (i.e. velocity at 90° to cylinder axis)	1	$k'b$			
Velocity gradient in longitudinal direction	$k'b$	$(k'b)^2$	$(k'b)^{-1}$	$(k'b)^{-1}$	1
Velocity gradient in transverse direction	$(k'b)^{-1}$	1			
Velocity potential	$k'b$	$(k'b)^2$	$k'b$	$k'b$	$(k'b)^2$

TABLE 1. The $k'b$-order of various constituents of the first-$k'a'$-order diffracted and radiated flow around a thin cylinder in waves

the cylinder with the free surface. The correct flow around a free-surface intersection can be realized from the above circular harmonics in two stages. First, we can add a three-dimensional potential flow which gives equal and opposite normal flow at the still-water position to that given by the circular harmonics. This flow will in general (for an oblique free-surface intersection) be of the same $k'b$-order as the transverse velocity in the circular harmonics, and since the distances involved (e.g. between the points of maximum and minimum potential) are again of order $k'b$, the flow is exactly analogous to that around a submerged cylinder end, as shown in table 1. Secondly, we can add a further three-dimensional potential flow so that the whole diffracted-plus-radiated potential satisfies the free-surface boundary condition (2.5), in which the second term had just been set to zero (by means of the flow in table 1 column 4), and the first was (see table 1) of order $k'b$. The further potential needed therefore satisfies (2.5) with minus this first term on the right-hand side, and since the distances involved are once more of order $k'b$, this second three-dimensional flow is in all respects one $k'b$-order higher than the first one, as shown in table 1.

Having completed our description of the general flow features around the cylinder, we now briefly examine the conventional next step (Lighthill 1979, equations 41–45) which is to calculate the fluid loads from the well-known pressure formula (see e.g. Batchelor 1967, equation 6.2.5)

$$-\rho\frac{\partial\phi}{\partial t}-\tfrac{1}{2}\rho\nabla\phi\cdot\nabla\phi, \tag{2.6}$$

where ρ is the fluid density. The first $k'a'$-order load can only come from the first term, since the second term involves the square of velocity and is thus of second $k'a'$-order. This paper addresses the limiting case of small $k'b$; our interest is therefore limited to the lowest-$k'b$-order terms in the wave load. We see in table 1 that our first-$k'a'$-order wave load from the diffracted and radiated flow will accordingly come

entirely from the first column; the other columns having velocity potentials which are either of a higher $k'b$-order, or affect a surface area of a higher $k'b$-order, or both. For our purposes the crucial point is the simple one that this first-$k'a'$-order wave load is of *second* order in $k'b$; because the velocity potential, as well as the surface areas involved, are of first $k'b$-order. The same applies to the remaining first-$k'a'$-order wave load from the incident flow, by the elementary argument that fluid pressure gradients produce forces on immersed bodies proportional to their volume, and thus in our case to their radius squared. When we consider the second-$k'a'$-order wave load, it turns out that this also is of second order in $k'b$; Lighthill (1979) therefore stresses the important conclusion that second-$k'a'$-order wave loads cannot be ignored for the limiting case of small-diameter cylinders (i.e. small $k'b$).

In investigating this point further, it should be noted that like Lighthill our concern will be with the *total* wave load, whether of first or second $k'a'$-order. For example, Lighthill showed that the second-$k'a'$-order wave force on his fixed vertical cylinder in regular waves is a pure second harmonic of the wave frequency (Lighthill 1979, equation 47), the second-$k'a'$-order steady force vanishing in comparison in the small-$k'b$ limit. So in this case we shall not be concerned with the details of the limiting properties of the steady force, or in particular with the work of McIver (1987) and Eatock-Taylor & Hung (1985), who have shown that in the small-$k'b$ limit the second-$k'a'$-order steady force on a group of fixed vertical cylinders is proportional to the square of the number of cylinders. For our purposes this is immaterial: it is sufficient that the ratio of the steady force to the second harmonic tends to zero with $k'b$, so that in this limit it makes zero contribution to the *total* second-$k'a'$-order wave load.

An important source of second-$k'a'$-order loads is the second term in (2.6) evaluated for the first-$k'a'$-order potential (Lighthill 1979, equation 33). This term is well-known to produce zero translational load in a uniform incident flow (D'Alembert's paradox, see e.g. Batchelor 1967). Lighthill showed that accordingly the effects of the lowest-$k'b$-order parts of the transverse velocity featured in column 1 of table 1 cancel out on their own, and it is necessary to consider the higher-$k'b$-order parts of the transverse velocity in column 2 resulting from the velocity gradient, and, interestingly, the $k'b$-order longitudinal velocity in column 1. The result is nevertheless a force of second $k'b$-order, and therefore significant for even the thinnest cylinders, as just highlighted, because the first-$k'a'$-order load is of second-$k'b$-order too. Applying this approach to more general examples than Lighthill's infinite vertical cylinder involve the special three-dimensional end flows in table 1 columns 3–5, since although the areas involved are clearly one $k'b$-order smaller than the main cylinder surface area, we see from table 1 that the fluid velocities are one $k'b$-order larger (given that the direct effects of the lowest-$k'b$-order parts of the transverse velocity in column 1 cancel, as we have just noted). Thus these end flows also produce second-$k'b$-order fluid loads, exactly comparable with Lighthill's loads from longitudinal flow and velocity gradients.

3. Two suggestive classical results

At first sight, therefore, the accurate calculation of potential-flow wave loading on thin cylinders is a matter of laborious consideration of the details of pressure distribution resulting from end effects, longitudinal diffracted flow, and incident-wave velocity gradients. So laborious, in fact, that there appears to be little realistic prospect of completing the task for the general case without error – recent attempts

have evidently (Angwin 1986) all required arbitrary approximations. There are, however, signs in the classical literature that the problem has a simpler structure: strikingly, Lamb (1932, §117) begins his chapter on the subject by remarking of Kelvin, Tait & Kirchhoff that 'The cardinal feature of the methods followed by these writers consists in this, that the solids and the fluid are treated as forming together one dynamical system, and thus the troublesome calculation of the effect of the fluid pressures on the surfaces of the solids is avoided.'

Two of the classical results given by Lamb after that remark are particularly suggestive when applied to our problem of thin cylinders. The first is the formula given by Kirchhoff (Lamb 1932, §124 equation 6) for the turning moment felt by a body in steady translation through still water (known in the later aeronautical literature as the 'Munk moment'), which in modern notation (Milne-Thomson 1968, §18.50 following Lamb exactly, or more accessibly Lighthill 1986*a*, equation 338) is $\boldsymbol{m} \wedge \boldsymbol{v}$ where $\boldsymbol{v}$ is the velocity and $\boldsymbol{m}$ the 'momentum' (i.e. added-mass matrix times velocity). This is clearly non-zero for a thin cylinder moving obliquely, i.e. translating in a straight line neither along, nor perpendicular to, its axis. But we see from table 1 that in this oblique case there is in fact no resultant fluid load along the length of the cylinder, because the longitudinal fluid velocity, as well as the transverse fluid velocity, are suitably symmetric around it. It therefore follows that the surface pressures causing the Munk moment must occur entirely at the ends of the cylinder, where there will be stagnation points and thus pressures high enough to offset the small end areas involved, as described in general formal terms at the end of §2.

At first sight, therefore, it appears that calculation of the Munk moment is not possible without careful consideration of the three-dimensional flow features at each end of the cylinder, in sufficient detail to determine the transverse fluid load at each end caused by the off-centre bias of the stagnation points in oblique flow. Remarkably, however, the Kirchhoff moment formula $\boldsymbol{m} \wedge \boldsymbol{v}$ is completely insensitive to these details – all that it requires is the transverse and longitudinal added masses, so as to give $\boldsymbol{m}$. And in the thin-cylinder limit the former is just the length times the two-dimensional added mass per unit length, and the latter tends to zero by comparison. This is because the end effects on the transverse added mass, and the entire longitudinal added mass, are proportional to the cube of the cylinder diameter, whereas the transverse added mass is proportional to the cylinder volume. See incidentally Lighthill's (1986*a*, §8.4) detailed treatment of a Rankine ovoid leading to the same conclusion; for our purposes it is sufficient to observe that the details of the three-dimensional flow at the cylinder ends are immaterial, since their contribution to $\boldsymbol{m}$ vanishes in the thin-cylinder limit.

The key to this apparent paradox clearly lies in Kirchhoff's deduction of fluid loads by a moment argument (Lamb 1932, §119) rather than by integrating surface pressures. From the momentum viewpoint the Munk moment is unconnected with end effects but is loosely speaking (see e.g. Lighthill 1986*a*, §8.4 for precise details) the result of the steadily arising angular momentum of the fluid about a distant-fluid-fixed axis, from which the line of action of $\boldsymbol{m}$ grows steadily more distant, because $\boldsymbol{m}$ is not parallel to $\boldsymbol{v}$. It appears, therefore, that *fewer flow details are required to calculate fluid loads on thin cylinders by a momentum argument, than by integration of surface pressures*, if this first simple example is anything to go by.

A related message comes from another simple example given by Lamb (1932, §143). This is Taylor's use of an energy argument to determine the fluid loads on a small body fixed in a non-uniform stream. Taylor (1928*b*) showed that a calculation

of the fluid kinetic energy assuming the stream to be *uniform* (Taylor 1928*b*, equation 5) was sufficient to deduce the fluid forces (although not the moments) arising from the stream's *non*-uniformity – the stream's velocity gradients reappearing correctly in his force expression via his energy position derivative. Taylor also calculated the fluid loads conventionally by surface pressure integration. Since the pressures around a body fixed in a uniform stream exert zero net force (D'Alembert's paradox), he had of necessity to analyse the flow details associated with the stream's non-uniformity (Taylor 1928*b*, equations 14, 18), using a method analogous to Lighthill's (2.3) and (2.4) above, but with simple spherical harmonics because the body was assumed small in all dimensions. For our purposes the important point is that although this level of detail was essential for the pressure argument, it was unnecessary for the energy, just as details of end flow were unnecessary for the momentum argument above. It therefore appears that *calculating fluid loads by energy arguments also requires fewer flow details than calculations from surface pressures*, if this second simple example is anything to go by.

These two classical results suggest that the modern problem of wave loading on a lattice structure might be fruitfully approached by classical momentum or energy arguments rather than the normal modern method of surface pressure integration, which appears to be prohibitively complex. The result derived below in fact uses the energy approach; from the simple vector form of the result, it could presumably also be derived by a momentum argument.

4. The approximation of an incident-wave-shaped 'lid'

The central approximation of this paper, which enables the energy argument to be used, is that *the position of the wave surface is unaffected by the presence of the structure*. Similar thinking has been loosely applied with Morison's equation for many years by the practice of applying it 'up to the incident wave surface' (implying that the height of the water surface around cylinder–surface intersections is in some average way equal to the incident wave height on the cylinder centreline): in this paper we make a precise assumption in that spirit by constraining the free surface with a 'wavy lid' to move exactly as it would if the structure were absent. In terms of the power series scheme developed in §2, this conveniently corresponds to omitting the free-surface-induced flow constituting the final column in table 1. This Section establishes the consequences of that omission on the various constituents of the total wave load on a lattice structure built of thin cylinders.

The key point about the omitted free-surface-induced flow (and indeed the flows of table 1 columns 3 and 4 too) has already been noted in §2; it is that the flow is a truly three-dimensional 'end effect' in that it only extends along the cylinder for a distance of order $k'b$, and hence affects a cylinder area of order only $(k'b)^2$. Since the fluid loads considered in §2 were shown there to be of order $(k'b)^2$ too, it follows that the contribution to this fluid load from the omitted flow vanishes in the thin-cylinder limit unless the pressures there are of *zeroth* order in $k'b$. We have already seen in §2 that its contribution to the first-$k'a'$-order fluid load (and indeed also the contribution to that load from the flows in columns 3 and 4 of table 1) vanishes in this way because the first-$k'a'$-order fluid pressures involved are higher than zeroth $k'b$-order. In this Section we extend that argument to see at what $k'a'$-order, if at all, the omitted free-surface-induced flow makes a contribution to the total fluid load in our thin-cylinder limit.

The second-$k'a'$-order free-surface boundary condition is (see e.g. Lighthill 1979, equation 25)

$$\frac{\partial^2\phi}{\partial t^2}+g\frac{\partial\phi}{\partial z}=-\frac{\partial}{\partial t}(q^2) \tag{4.1}$$

applied at the instantaneous free surface, where q is the amplitude of the total first-$k'a'$-order fluid velocity. A cylinder intersecting the surface produces zeroth-$k'b$-order changes to the right-hand side (from what it would be without the cylinder present), see table 1, and so must produce a second-$k'a'$-order free-surface-induced flow (i.e. a second-$k'a'$-order flow omitted by our wavy-lid approximation) with velocities also of zeroth $k'b$-order. This will make it resemble in all its $k'b$-orders the flows in table 1 columns 3 and 4; in this way the first term on the left-hand side will be of first $k'b$-order and the second of zeroth $k'b$-order, giving the required overall zeroth $k'b$-order for the left-hand side. It is striking that the second-$k'a'$-order free-surface-induced flow is in all respects an order *lower* in $k'b$ than the first-$k'a'$-order free-surface-induced flow, see table 1 column 5.

Nevertheless, because the second-$k'a'$-order load from this omitted second-$k'a'$-order flow comes via the first term in (2.6) (the second term being of higher $k'a'$-order), the pressures in question are of first $k'b$-order (like the velocity potential, see table 1 columns 3 and 4), and so fail to meet the requirement above for a zeroth-$k'b$-order pressure. Thus not only does our wavy-lid approximation not affect the first-$k'a'$-order fluid load in the thin-cylinder limit, it *does not affect the second-$k'a'$-order fluid load either*. This important conclusion can be checked, if desired, by the mechanical route of examining in turn the list of second-$k'a'$-order wave loading terms on a moving structure usually credited to Pinkster (1979) (although his original list is incomplete, see Standing, Dacunha & Matten 1981, confirmed e.g. by Mavrakos 1988). The first such term is the total load from the second-$k'a'$-order potential as a whole, which on the Pinkster view will be partly present anyway in the incident waves, and partly generated by second-$k'a'$-order errors in the cylinder-surface boundary condition. The above argument would then just be used to show that the *perturbation* to this load produced by the wavy lid vanishes for small $k'b$. The remainder of the second-$k'a'$-order load would be considered as the sum of various product terms of first-$k'a'$-order quantities (e.g. the effects of the second term in (2.6) evaluated for first-$k'a'$-order velocity, as described in §2), which can all be readily seen to be unaffected in the thin-cylinder limit, because the first-$k'a'$-order flow which has been omitted has a suitably high $k'b$-order (see table 1 column 5) and/or acts over an area of order $(k'b)^2$, as already noted.

The general features of the second-$k'a'$-order free-surface-induced flow established above also reveal where the first effects of the wavy-lid approximation are felt, which is at third order in $k'a'$. This because at third $k'a'$-order the second pressure term in (2.6) must be evaluated using a velocity expression correct to second $k'a'$-order, and must therefore include a contribution from this free-surface-induced flow, which would be omitted by our wavy-lid approximation. The squaring process in the pressure term will produce third-$k'a'$-order product terms between this free-surface-induced velocity and the first-$k'a'$-order velocity: because both of these are of zeroth $k'b$-order (see above and table 1), their product will be of the zeroth $k'b$-order required above.

From a practical point of view the fact that our wavy lid introduces no error to second $k'a'$-order is mainly of computational interest (although there are a restricted class of pure second-$k'a'$-order practical problems, see e.g. Rainey 1986 and Pinkster 1979) because it means that computer programs using this approximation can be

debugged by comparison with second-$k'a'$-order parameters calculated by other means. However, the fact that the error occurs at third (rather than, say, fourth) $k'a'$-order is academic compared to the fact stressed above that the error is a *localized* pressure anomaly, at the intersection point of cylinders with the free surface. This is because most practical problems of nonlinear wave loading on lattice-type offshore structures involve some kind of gross nonlinearity, such as the intermittent immersion of a whole structural member, or the structure moving to some completely new mean attitude. In these circumstances the Stokes' expansion procedure of power series expansion about a nominal mean position (of the water surface and/or the structure) breaks down, and with it the concept of the $k'a'$-order of errors. However, the wavy-lid approximation can still be used with confidence, in the knowledge that the only errors introduced are localized to the free-surface intersection – elsewhere no approximation is being made at all, except that the cylinders are thin. Indeed, if these localized errors are of particular concern, then the second-$k'a'$-order approximation to the fluid load from 'end effects' at the surface intersections can be calculated from the formula (7.4) below, and any modifications to it considered.

5. An expression for the fluid kinetic energy

The wavy-lid approximation, together with the limiting flow properties listed in table 1, give a remarkably simple formula for the fluid kinetic energy. This was anticipated in §3, and the result is reminiscent of Taylor's (1928*a*, *b*) simple energy formulae referred to there, although the contexts and arguments are quite different.

The first critical point, as in Taylor (1928*b*), is to define precise 'conditions at infinity', for otherwise a moving fluid extending to infinity may easily possess infinite kinetic energy. Taylor's (1928*b*) device of a 'fluid circulating in a cyclic space', for which the energy formulae were derived by Kelvin, cannot be used here if only because the immersed volume of our lattice structures is not constant. Instead, we can envisage the structure acted on by a 'local storm', in an ocean of infinite depth, as shown in figure 1 (which also defines the volumes V, D, the surfaces S, S', the line-network L, the point R, the angle α, and the vectors $\boldsymbol{r}, \boldsymbol{n}, \boldsymbol{l}, \boldsymbol{n}', \boldsymbol{t}$). Even the varying immersion of the structure is then no problem, because from a far enough distance the storm and structure will appear as at most a three-dimensional monopole source, and thus impart finite kinetic energy to the fluid. (Of course, since our final loading equation in §6 depends only on local flow properties it is not limited to water of infinite depth – just as Taylor's result is, as he argues (Taylor 1928*b*, 'Previous Work'), not limited to flow in a cyclic space. We are considering the limiting case of small cylinder diameter with the water depth held fixed, which is closely analogous to Taylor's limiting case of small body dimensions with the width of the cyclic channel held fixed.) Writing $\phi_{\mathrm{D+R}}$ for the diffracted-plus-radiated velocity potential, we can thus write the total fluid kinetic energy e as

$$e = \tfrac{1}{2}\rho \int_V \nabla(\phi_{\mathrm{I}} + \phi_{\mathrm{D+R}}) \cdot \nabla(\phi_{\mathrm{I}} + \phi_{\mathrm{D+R}}) \tag{5.1}$$

$$= \tfrac{1}{2}\rho \int_V \nabla\phi_{\mathrm{I}} \cdot \nabla\phi_{\mathrm{I}} + \tfrac{1}{2}\rho \int_V (2\nabla\phi_{\mathrm{I}} + \nabla\phi_{\mathrm{D+R}}) \cdot \nabla\phi_{\mathrm{D+R}}. \tag{5.2}$$

There is no restriction to any $k'a'$-order or $k'b$-order in this expression: ϕ_{I} is now unconditionally the potential of the incident waves, and $\phi_{\mathrm{D+R}}$ just satisfies the wavy-lid approximation.

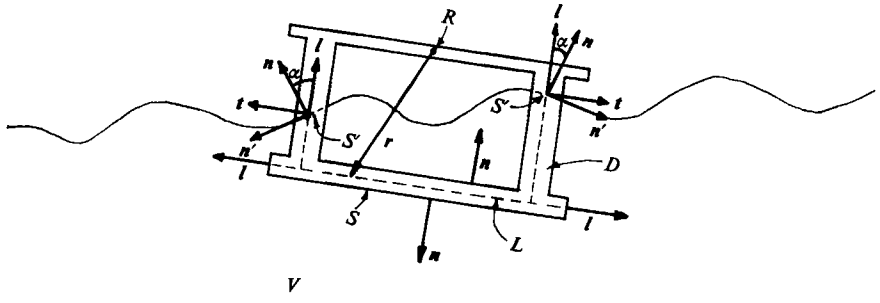

FIGURE 1. Definition sketch. The water surface shown is, crucially, in the same position it would occupy were the structure absent, and the waves are only a 'local storm', with the water surface becoming flat after some large but finite distance. S' is the portion of the undisturbed wave surface within the structure; taken together with the wetted surface S of the structure, it encloses a volume D and has a surface normal $\boldsymbol{n}$ (pointing out of D). The member centrelines L within D are continued by the unit vectors $\boldsymbol{l}$ at their ends. On S', $\boldsymbol{t}$ is the normal to $\boldsymbol{l}$, and $\boldsymbol{n}'$ the normal to $\boldsymbol{n}$, all four being in the same plane with $\boldsymbol{t}\cdot\boldsymbol{n} > 0$, $\boldsymbol{t}\cdot\boldsymbol{n}' > 0$. Finally R is a reference point fixed within the structure, $\boldsymbol{r}$ is position relative to it, and V is the volume of water outside D, stretching to infinity.

We now require a small technical lemma, which is that either of our potentials ϕ satisfy

$$\int_V \nabla\phi\cdot\nabla\phi_{\mathrm{D+R}} = \int_D \nabla\phi\cdot(\boldsymbol{v}-\boldsymbol{u}) - \int_{S'} \phi(\boldsymbol{v}-\boldsymbol{u})\cdot\boldsymbol{n}, \tag{5.3}$$

where $\boldsymbol{v} = \nabla\phi_{\mathrm{I}}$ is the incident velocity and $\boldsymbol{u} = \boldsymbol{v}+\boldsymbol{\omega}\wedge\boldsymbol{r}$ is the local structural velocity ($\boldsymbol{\omega}$ being the angular velocity of the structure, and $\boldsymbol{v}$ its velocity at R). The definition of the potential ϕ *inside* the structure is no problem if ϕ is ϕ_{I}; if it is $\phi_{\mathrm{D+R}}$ then we must define it by making it (but not its derivatives) continuous over S, and giving it zero normal derivative over S', as it has over the lid. These mixed boundary conditions over the surface of D are sufficient to define $\phi_{\mathrm{D+R}}$ uniquely within D, see e.g. Batchelor (1967, p. 103). The proof of our small lemma is elementary, because the left-hand side can be transformed with Green's theorem to

$$-\int_S \phi\nabla\phi_{\mathrm{D+R}}\cdot\boldsymbol{n} = -\int_S \phi(-\boldsymbol{v}+\boldsymbol{u})\cdot\boldsymbol{n}, \tag{5.4}$$

the surface S being sufficient because $\nabla\phi_{\mathrm{D+R}}\cdot\boldsymbol{n}$ is by definition zero on the wavy lid, and the similar contribution from a far hemisphere centred on the local storm is zero because ϕ and $\nabla\phi_{\mathrm{D+R}}$ in combination decay sufficiently rapidly with distance. This in turn can be transformed with Gauss' theorem to

$$\int_D \nabla\phi\cdot(\boldsymbol{v}-\boldsymbol{u}) + \int_D \phi(\nabla\cdot\boldsymbol{v}-\nabla\cdot\boldsymbol{u}) - \int_{S'} \phi(\boldsymbol{v}-\boldsymbol{u})\cdot\boldsymbol{n}, \tag{5.5}$$

in which the second term vanishes because $\nabla\cdot\boldsymbol{v}$ and $\nabla\cdot\boldsymbol{u}$ are both zero. (In this paper the use of the symbol ∇ follows Batchelor 1967, p. xviii.)

Applying this result to the second term in (5.2), and expressing the first term as the kinetic energy in the undisturbed incident wave, e_{I}, minus an integral over D, gives

$$e = e_{\mathrm{I}} - \tfrac{1}{2}\rho\int_D \boldsymbol{v}\cdot\boldsymbol{v} + \tfrac{1}{2}\rho\int_D (2\boldsymbol{v}+\nabla\phi_{\mathrm{D+R}})\cdot(\boldsymbol{v}-\boldsymbol{u}) - \tfrac{1}{2}\rho\int_{S'} (2\phi_{\mathrm{I}}+\phi_{\mathrm{D+R}})(\boldsymbol{v}-\boldsymbol{u})\cdot\boldsymbol{n}. \tag{5.6}$$

The remarkable property of this expression is its simplicity in the limit of small $k'b$, even for the general case of a lattice structure with complex joints. For we see at once that the first integral must become in this limit

$$-\tfrac{1}{2}\rho \int_L c\boldsymbol{v}\cdot\boldsymbol{v}, \tag{5.7}$$

where c is the local cylinder cross-sectional area, because the gradients of $\boldsymbol{v}$ will from (2.2) clearly produce a contribution of higher order in $k'b'$, and there are clearly no complexities at ends or joints. Also the last integral will become in this limit

$$-\rho \sum_p \phi_{\mathrm{I}}(\boldsymbol{v}-\boldsymbol{u})\cdot\boldsymbol{n}c/\cos\alpha, \tag{5.8}$$

where, see figure 1, α is the local angle (to the perpendicular) at which L meets S', and Σ_p indicates the summation over all intersection points of the structure with the water surface. This is because gradients of ϕ_{I} similarly produce contributions of higher order in $k'b$, as does $\phi_{\mathrm{D+R}}$ (see table 1). We note incidentally that the $\cos\alpha$ term in (5.8) prohibits the consideration of exactly tangential surface intersections ($\alpha = 90°$); it can be argued that the probability of this event is zero, and comparisons are precluded with the classical idealized problem of the partially immersed horizontal cylinder. Finally, in the limit of small $k'b$ the second integral will become

$$\frac{1}{2}\int_L \{2\rho c\boldsymbol{v}+\boldsymbol{m}(\boldsymbol{v}-\boldsymbol{u})\}\cdot(\boldsymbol{v}-\boldsymbol{u}), \tag{5.9}$$

where $\boldsymbol{m}$ is the local two-dimensional added-mass-per-unit-length mapping of structural members, considered as a three-dimensional mapping (i.e. the mapping which sets longitudinal components to zero, and multiplies transverse components along the principal added-mass axes by the appropriate added masses). This is because $\nabla\phi_{\mathrm{D+R}}$ is dominated at small $k'b$ by the cylinder's reaction to the incident velocity and the effects of its motion, the contribution from the incident velocity gradients and higher velocity position derivatives vanishing by comparison as $k'b$ tends to zero (see (2.4)); the case of a circular cylinder is particularly simple because in the small-$k'b$ limit $\nabla\phi_{\mathrm{D+R}}$ inside the cylinder is simply the transverse component of $(\boldsymbol{v}-\boldsymbol{u})$.

On a broader view, perhaps, there is nothing surprising about these simple limiting forms, which are merely a matter of the obvious dominant terms dominating. Rather, it was by contrast a surprisingly complex matter to find in §2 the limiting form of the surface integral of the second pressure term in (2.6), because the obvious dominant terms cancelled out (D'Alembert's paradox), leaving a complex variety of 'runners up' requiring a particularly detailed study of the flow, as highlighted in §3. In any event, it is now convenient to gather the incident, radiated, and product terms in our limiting fluid energy expression, thus

$$e = \left[e_{\mathrm{I}}+\frac{1}{2}\int_L \boldsymbol{v}\cdot(\boldsymbol{m}+\rho c)\,\boldsymbol{v}-\rho\sum_p \phi_{\mathrm{I}}\,\boldsymbol{v}\cdot\boldsymbol{n}c/\cos\alpha\right]+\left[-\int_L \boldsymbol{u}\cdot(\boldsymbol{m}+\rho c)\,\boldsymbol{v}\right.$$
$$\left.+\rho\sum_p \phi_{\mathrm{I}}\,\boldsymbol{u}\cdot\boldsymbol{n}c/\cos\alpha\right]+\frac{1}{2}\int_L \boldsymbol{u}\cdot\boldsymbol{m}\boldsymbol{u}. \tag{5.10}$$

By writing $\boldsymbol{u}$ as $\boldsymbol{v}+\boldsymbol{\omega}\wedge\boldsymbol{r}$, then collecting terms with suitable arrangement of the scalar triple products, we can write this in the form

$$e = e_{\mathrm{F}}+\boldsymbol{I}\cdot\boldsymbol{U}+\tfrac{1}{2}\boldsymbol{U}\cdot\boldsymbol{M}\boldsymbol{U}, \tag{5.11}$$

where U is the six-dimensional vector $(\boldsymbol{v}, \boldsymbol{\omega})$. Here obviously the 'fixed-structure fluid kinetic energy' e_F is given by

$$e_F = e_I + \frac{1}{2}\int_L \boldsymbol{v}\cdot\boldsymbol{m}'\boldsymbol{v} - \rho\sum_p \phi_I \boldsymbol{v}\cdot\boldsymbol{n}c/\cos\alpha, \tag{5.12}$$

where we are economizing by writing $\boldsymbol{m}' = \boldsymbol{m} + \rho c$. The six-dimensional vector $\boldsymbol{I}$ is given by

$$\boldsymbol{I} = \left\{\left(-\int_L \boldsymbol{m}'\boldsymbol{v} + \rho\sum_p \phi_I \boldsymbol{n}c/\cos\alpha\right), \left(-\int_L \boldsymbol{r}\boldsymbol{m}'\boldsymbol{v} + \rho\sum_p \phi_I \boldsymbol{r}\boldsymbol{n}c/\cos\alpha\right)\right\} \tag{5.13}$$

where we are economizing by writing $\boldsymbol{r}\wedge$ as the three-dimensional linear mapping $\boldsymbol{r}$. The 'added mass' six-dimensional linear mapping is given by

$$\boldsymbol{M} = \int_L \begin{Bmatrix} \boldsymbol{m} & -\boldsymbol{m}\boldsymbol{r} \\ \boldsymbol{r}\boldsymbol{m} & \boldsymbol{r}\boldsymbol{m}\boldsymbol{r} \end{Bmatrix}. \tag{5.14}$$

Since $\boldsymbol{m}$ is symmetric and $\boldsymbol{r}$ is skew-symmetric, $\boldsymbol{M}$ is of course symmetric overall. It also obviously ignores the longitudinal added masses of the cylinders, because in the small-$k'b$ limit they are vanishingly small relative to their transverse added masses, as described in §3.

6. The equation of motion

From the fluid kinetic energy, Taylor (1928*b*, equations 2, 3) deduced the fluid loading on a small body fixed in steady flow by the simple observation that the change in this kinetic energy after a notional displacement of the structure must equal the work done against the fluid loading during the notional displacement. Strikingly, if that argument is applied to our kinetic energy expression (which for a fully immersed fixed structure reduces to just the first two terms in (5.12)), then it gives *minus* the loading deduced by Taylor (cf. Taylor 1928*b*, equation 2). This shows the importance of the 'conditions at infinity' – Taylor's argument relies on the fixed walls of Kelvin's cyclic space doing no work; with our moving wavy lid the argument collapses. This is because it is well known that the reaction at the fluid walls to an accelerating immersed body does not fall to zero as the walls are made more distant (the basis of the famous lack of convergence of the fluid momentum integral, Lamb, 1932 §119); in our case this may be simply seen from the fact that useful work can be extracted by moving our structure cyclically with a suitable phase relative to the waves – there must therefore be a corresponding work input on the wavy lid.

However, there are no problems with Kelvin's more general Lagrange-equation argument alluded to by Taylor (1928*b*) and proved independently by Lamb (1932, §§135, 136). We simply take advantage of the fact that our wavy lid has suppressed all the degrees of freedom of the problem except six generalized rigid-body position coordinates q_i of the structure, and write down Lagrange's equations using our kinetic energy expression (5.11):

$$\frac{\mathrm{d}}{\mathrm{d}t}\left\{\frac{\partial}{\partial\dot{q}_i}(\boldsymbol{I}\cdot\boldsymbol{U} + \tfrac{1}{2}\boldsymbol{U}\cdot\boldsymbol{M}^*\boldsymbol{U})\right\} - \frac{\partial}{\partial q_i}\{e_F + \boldsymbol{I}\cdot\boldsymbol{U} + \tfrac{1}{2}\boldsymbol{U}\cdot\boldsymbol{M}^*\boldsymbol{U}\} = f_i \tag{6.1}$$

To (5.11) we have added the structural kinetic energy by replacing the added mass $\boldsymbol{M}$ by the total mass $\boldsymbol{M}^*$, and can omit e_F from the first term above since clearly $\partial e_F/\partial\dot{q}_i = 0$. Lastly, the generalized force and moment from all non-hydrodynamic sources is written f_i. Incidentally, another consequence of the suppression of the fluid

surface degrees of freedom is that henceforth we are dealing with fully nonlinear ordinary differential equations of motion, and so have access to the formidable new results and methods of dynamic systems theory (see Thompson & Stewart 1986). This contrasts with numerical methods in which the surface freedoms are retained (the third approach of §1), for which there is no comparable insight available into their likely behaviour in any particular case.

The usefulness of (6.1) can be greatly enhanced because the simplicity of the energy expression allows the generalized coordinates to be systematically eliminated. This is done in Appendix B, and results in

$$\frac{\mathrm{d}}{\mathrm{d}t}(\boldsymbol{I}+\boldsymbol{N})+\{0,(\boldsymbol{k}+\boldsymbol{h})\wedge\boldsymbol{\omega}\}=\frac{\partial}{\partial \boldsymbol{X}}(e_{\mathrm{F}}+\boldsymbol{I}\cdot\boldsymbol{U}+\tfrac{1}{2}\boldsymbol{U}\cdot\boldsymbol{M}^{*}\boldsymbol{U})+\boldsymbol{Q}, \tag{6.2}$$

where we are writing $\boldsymbol{M}^{*}\boldsymbol{U}$ as $\boldsymbol{N}=(\boldsymbol{m},\boldsymbol{h})$ (this quantity would classically be known as the 'impulse' of the structure (Lamb 1932, §119), the hydrodynamic part being, via (5.4), the integral of the radiated potential over the structure's wetted surface) and similarly writing $\boldsymbol{I}=(\boldsymbol{j},\boldsymbol{k})$ (this quantity can analogously be called the 'wave impulse', being a similar integral of the incident plus diffracted potentials, i.e. the impulsive pressures on the structure due to the waves). Lastly, we are writing $\boldsymbol{Q}$ for the non-hydrodynamic force (acting at R) and moment on the structure. In particular, $\boldsymbol{Q}$ includes the effect of gravity, which has hitherto been ignored because with our wavy lid we have a perfectly well-defined problem without it. Gravity will simply produce an additional force (the structure's weight) acting at its centre of gravity, and an additional hydrostatic pressure in the fluid, equal to ρg times the vertical distance below the position of the undisturbed water surface. The resulting hydrostatic force (acting at R) and moment on the structure is its integral over the wetted surface of the structure, which can be transformed with Gauss' theorem (cf. (5.5), this time the gradient of the pressure is $\rho\boldsymbol{g}$, where $\boldsymbol{g}$ is the vector acceleration due to gravity, acting downwards) to a volume integral whose limiting form for thin cylinders (cf. (5.7), (5.8)) is

$$-\rho\int_{L}c(\boldsymbol{g},\boldsymbol{r}\wedge\boldsymbol{g})-\sum_{p}\rho g\eta c/\cos\alpha(\boldsymbol{n},\boldsymbol{r}\wedge\boldsymbol{n}), \tag{6.3}$$

where η is the water surface elevation above its undisturbed position. (In practice some care is needed in the definition of the mean surface elevation, to ensure that the surface pressure on the undisturbed wave is zero as it should be. If the pressure at great depth is assumed to be unaffected by the waves, then the water surface must have a second-$k'a'$-order mean 'set down' to achieve this. Alternatively, if the mean surface position is taken as fixed, as it would be in a model basin, then the pressure at great depth must be increased.) The second term is noteworthy: it only vanishes if the structure is fully immersed or the water is still, so that (6.3) is only equal to the Archimidean definition of $-\rho\boldsymbol{g}$ times immersed volume (i.e. the first term in (6.3)) in those special cases.

In order to bring out the relationship of (6.2) to the classical results for the simple case of a moving body fully immersed in an unbounded expanse of still water, it is helpful to change to a special definition of the operator $\partial/\partial\boldsymbol{X}$. This is because in that situation the expression $e_{\mathrm{F}}+\boldsymbol{I}\cdot\boldsymbol{U}+\frac{1}{2}\boldsymbol{U}\cdot\boldsymbol{M}^{*}\boldsymbol{U}$ (i.e. the total kinetic energy of fluid and structure) clearly does not vary with $\boldsymbol{X}$, provided the velocity $\boldsymbol{U}$ maintains its amplitude and orientation relative to the structure. The operator $\partial/\partial\boldsymbol{X}$ by contrast assumes that $\boldsymbol{U}$ is held fixed *in space* during the incremental changes in $\boldsymbol{X}$; if we

switch to an operator $\Delta/\Delta \boldsymbol{X}$ which assumes that $\boldsymbol{U}$ is held fixed *relative to the structure* during incremental changes of $\boldsymbol{X}$, our derivative term will conveniently vanish for that simple still-water case. Classically (Lamb 1932, §120) this type of argument would be persued by writing $\boldsymbol{U}$ in explicit components u_i in a space-fixed axis system, and explicit components μ_i in a body-fixed axis system – if we write our six position coordinates as x_i when u_i are understood to be the other variables, and as χ_i when μ_i are, then the required change is then simply from $\partial/\partial x_i$ to $\partial/\partial \chi_i$. Maintaining our coordinate-free vector notation, however, we can write an incremental position change as $\delta \boldsymbol{X} = (\delta \boldsymbol{x}_1, \delta \boldsymbol{x}_2)$, so that when $\boldsymbol{U}$ is held fixed relative to the structure, our position increment will cause it to change by

$$\delta \boldsymbol{U} = (\delta \boldsymbol{x}_2 \wedge \boldsymbol{v}, \delta \boldsymbol{x}_2 \wedge \boldsymbol{\omega}) \tag{6.4}$$

The associated change in the arbitrary variable f (cf. (B 2)) is therefore

$$\frac{\Delta f}{\Delta \boldsymbol{X}} \cdot \delta \boldsymbol{X} = \frac{\partial f}{\partial \boldsymbol{X}} \cdot \delta \boldsymbol{X} + \frac{\partial f}{\partial \boldsymbol{U}} \cdot (\delta \boldsymbol{x}_2 \wedge \boldsymbol{v}, \delta \boldsymbol{x}_2 \wedge \boldsymbol{\omega}). \tag{6.5}$$

Writing $\partial f/\partial \boldsymbol{U} = (\partial f/\partial \boldsymbol{v}, \partial f/\partial \boldsymbol{\omega})$, and rearranging the scalar triple products, this gives:

$$\frac{\Delta}{\Delta \boldsymbol{X}} = \frac{\partial}{\partial \boldsymbol{X}} + \left\{0, \left(\boldsymbol{v} \wedge \frac{\partial}{\partial \boldsymbol{v}} + \boldsymbol{\omega} \wedge \frac{\partial}{\partial \boldsymbol{\omega}}\right)\right\}. \tag{6.6}$$

Thus in the new notation our equation of motion (6.2) becomes

$$\frac{\mathrm{d}}{\mathrm{d}t}(\boldsymbol{I} + \boldsymbol{N}) + \{0, \boldsymbol{v} \wedge (\boldsymbol{m} + \boldsymbol{j})\} = \frac{\Delta e}{\Delta \boldsymbol{X}} + \boldsymbol{Q}, \tag{6.7}$$

where we are able to omit the structure's own kinetic energy from the $\boldsymbol{U} \cdot \boldsymbol{M}^* \boldsymbol{U}$ term (since it is always a constant if $\boldsymbol{U}$ is held fixed relative to the structure), leaving simply $\Delta e/\Delta \boldsymbol{X}$. We shall write this henceforth in the form

$$\frac{\mathrm{d}\boldsymbol{N}}{\mathrm{d}t} = \boldsymbol{Q} - \frac{\mathrm{d}\boldsymbol{I}}{\mathrm{d}t} + \{0, (\boldsymbol{m} + \boldsymbol{j}) \wedge \boldsymbol{v}\} + \frac{\Delta e}{\Delta \boldsymbol{X}} \tag{6.8}$$

so that the terms on the right-hand side can later be identified as various types of wave load on the structure.

Given the wavy-lid approximaton, (6.8) is equally true for an arbitrarily shaped body (see Rainey 1984), because the fluid kinetic energy will in general have a quadratic form like (5.11), although of course the terms in (5.11) will no longer be given by the simple thin-cylinder expressions (5.12)–(5.14), but by general surface integrals. In particular, if the body is moving in an unbounded expanse of still water, then $\boldsymbol{I}$ is zero and $\boldsymbol{N}$ is the classical 'impulse' of the body (Lamb 1932, §119), and (6.8) becomes equivalent, as it should be, to the classical Kirchhoff general equations of motion (Lamb 1932, §124; or in modern notation Milne-Thomson 1968, §18.43). These equations are derived by a quite different argument, based on momentum (as highlighted in §3), which is applicable only in an unbounded fluid: they are, however, just (6.8) with $\boldsymbol{N}$ written as $\partial/\partial \boldsymbol{U}(\frac{1}{2}\boldsymbol{U} \cdot \boldsymbol{M}^* \boldsymbol{U})$, and $\mathrm{d}/\mathrm{d}t$ expressed as a derivative in a body-fixed frame, plus $(\boldsymbol{\omega} \wedge \boldsymbol{m}, \boldsymbol{\omega} \wedge \boldsymbol{h})$. It can also be shown (Rainey 1984) that if the body is moving in an unbounded expanse of uniformly moving water, then (6.8) gives, as it should, exactly the same fluid loads as would be obtained by applying the Kirchhoff general equations in a frame moving with the far fluid.

A final refinement is to find an explicit expression for $\Delta e/\Delta \boldsymbol{X}$ in the thin cylinder (small $k'b$) limit – this is not strictly necessary, since $\Delta e/\Delta \boldsymbol{X}$ can be evaluated

computationally by comparing values of e at adjacent points, but is convenient for the comparisons of the next Section, and also saves computing time. It is done in Appendix C, which gives

$$\frac{\Delta e}{\Delta \boldsymbol{X}} = \int_L \{\boldsymbol{v}\boldsymbol{m}'(\boldsymbol{v}-\boldsymbol{u}), [\boldsymbol{r}\boldsymbol{v}\boldsymbol{m}'(\boldsymbol{v}-\boldsymbol{u}) - \boldsymbol{v} \wedge \boldsymbol{m}'(\boldsymbol{v}-\boldsymbol{u})]\} + \sum_p \boldsymbol{S}, \tag{6.9}$$

where $\boldsymbol{S}$ is a 6-vector defined there, and $\boldsymbol{v}$ is the velocity gradient mapping (i.e. $\boldsymbol{v}$ gives the change in $\boldsymbol{v}$ over a small displacement $\boldsymbol{\delta}$ as $\boldsymbol{v}\boldsymbol{\delta}$). The complexity of the expressions for $\boldsymbol{S}$ do detract somewhat from the simplicity of (6.8), and may be thought therefore to reduce the reliability of computer programs based on it – such programs can however be made self-checking by also evaluating e, and continuously comparing δe with $(\Delta e/\Delta \boldsymbol{X})\cdot\delta \boldsymbol{X}$, making due allowance for $\delta \boldsymbol{U}$.

A final computational point is that the expression (6.9) clearly does not apply at those discrete instants when the end of a cylinder is crossing the water surface, for then there is a step change in e of $\rho\phi_{\mathrm{I}}(\boldsymbol{v}-\boldsymbol{u})\cdot\boldsymbol{n}c/\cos\alpha$ (see (5.8)), which will give very large loads $\Delta e/\Delta \boldsymbol{X}$ on the right-hand side of (6.8), and be registered as an inconsistency by this self-checking routine. Simultaneously, however, there is a step change of $\rho\phi_{\mathrm{I}}(\boldsymbol{n}, \boldsymbol{r} \wedge \boldsymbol{n})c/\cos\alpha$ in $\boldsymbol{I}$ (see (5.13)), giving similar very large loads $\mathrm{d}\boldsymbol{I}/\mathrm{d}t$ on the right-hand side of (6.8). If we imagine these sudden changes in e and $\boldsymbol{I}$ to be occurring not instantaneously but linearly with penetration through a surface layer of arbitrarily small thickness ϵ, it is easy to show that the two large loads are both equal to $\epsilon^{-1}\rho\phi_{\mathrm{I}}(\boldsymbol{v}-\boldsymbol{u})\cdot\boldsymbol{n}(\boldsymbol{n}, \boldsymbol{r} \wedge \boldsymbol{n})c/\cos\alpha$, with the signs such that they cancel eaeh other out, giving zero net impulse. This is of course also necessary for physical consistency, since the right-hand side of (6.8) would certainly have given no impulse had we chosen a point on the water surface where $\phi_{\mathrm{I}} = 0$. In any event, it is necessary computationally to invoke this absence of an impulse during surface transits of cylinder ends, and simply hold the structural velocity constant for the single timestep involved, temporarily suspending the calculation of the right-hand side of (6.8).

7. Comparison with 'Morison's equation'

It has already been noted in §6 that in the fully immersed still-water case our whole equation of motion (6.8) can be identified as the classical Kirchhoff equations for an arbitrarily shaped body. We now compare (6.8) with the modern language of fluid loading on lattice-type offshore structures, in which fluid loads are described by the semi-empirical Morison's equation that gives the local lateral force per unit length as (see e.g. Sarpkaya & Isaacson 1981, equation 5.43)

$$\rho c[c_m \dot{v}_{\mathrm{T}} - (c_m - 1)\dot{u}_{\mathrm{T}}] + \rho b c_d (v_{\mathrm{T}} - u_{\mathrm{T}})\,|(v_{\mathrm{T}} - u_{\mathrm{T}})|, \tag{7.1}$$

where $(\,)_{\mathrm{T}}$ indicates the transverse component (considered as a scalar, e.g. $\dot{u}_{\mathrm{T}}$ is considered to be zero if u_{T} is constant in magnitude but changing in direction as the cylinder moves), and c_m and c_d are empirically adjusted coefficients. This paper is concerned with the potential-flow load only: it is easy to show that when the flow is uniform and two-dimensional (as in a U-tube apparatus), the potential-flow load is given exactly by the inertial (first) term in (7.1) (with $c_m = 2.0$ for a circular cylinder). We shall therefore be concerned with the non-uniform and three-dimensional potential-flow effects on a real structure in waves, which have already been identified in §2 as (i) end effects around submerged ends and free-surface intersections, see table 1 columns 3–5. In either case the effects can be categorized as

either steady flow or unsteady flow; (ii) longitudinal diffracted/radiated flow effects, see table 1 column 1 row 1; (iii) direct effects of incident velocity gradients, see table 1 column 2. In all cases the fluid load is calculated correctly by (6.8); we shall now perform this calculation in appropriate simple cases, first to cross-check the results with earlier calculations by other methods where available, and secondly to establish the conditions under which these calculations are practically significant at present. By this we mean the conditions under which the three-dimensional potential-flow load is significant even in the context of the other current uncertainties, particularly over the vorticity-induced load, which is currently calculated in a relatively crude two-dimensional fashion using the drag (second) term in Morison's equation (7.1). Since such a two-dimensional calculation of vorticity-induced load is in general an overestimate compared with the true three-dimensional effect (J. M. R. Graham 1987, private communication), our criterion for significance will be that (for a circular cylinder) our load be comparable with the *total* load predicted by Morison's equation, with $c_m = 2$ and $c_d = 1$ (typical of current practice).

7.1. *Steady-flow end effects*

The simplest case to consider is a fully immersed finite cylinder in steady translation in still water, as featured in §3: the only non-zero fluid loading term on the right-hand side of (6.8) is the Munk moment $\boldsymbol{m} \wedge \boldsymbol{v}$, which must be counteracted by an equal and opposite external couple $\boldsymbol{Q}$, since the left-hand side is zero. We saw in §3 that there is in fact no resultant fluid load along the length of the cylinder, so the Munk moment must be caused by end effects, which evidently must be giving a transverse force at each end of

$$-(\boldsymbol{u}\cdot\boldsymbol{l})\,\boldsymbol{mu}. \tag{7.2}$$

The next simplest case is a partially immersed cylinder in steady translation through the surface of still water, with one end out and one in. This time the left-hand side of (6.8) is not zero but is equivalent to a localized fluid force at the surface intersection of $(\boldsymbol{u}\cdot\boldsymbol{n})\,\boldsymbol{mu}/\cos\alpha$ on the right-hand side of (6.8). The $\Delta e/\Delta X$ term of (6.8) is also non-zero and gives via (C 5) another fluid force of $-\frac{1}{2}(\boldsymbol{u}\cdot\boldsymbol{mu})\,\boldsymbol{n}/\cos\alpha$ at the same location. Finally there is a Munk moment $\boldsymbol{m} \wedge \boldsymbol{v}$ as above, this time based on the instantaneous value of $\boldsymbol{m}$; since the transverse force at the immersed end must still be (7.2) above, we can represent the Munk moment by adding a similar force at the free surface. Taken together these free-surface forces have a longitudinal component which can only mean that there is a longitudinal force on the immersed end, viz.

$$\tfrac{1}{2}(\boldsymbol{u}\cdot\boldsymbol{mu})\,\boldsymbol{l}. \tag{7.3}$$

It may at first sight appear strange that this longitudinal force is zero if the cylinder velocity is purely longitudinal (in contrast to the force on the upstream half of a translating sphere of the same cross-section c, which from Batchelor (1967, equation 6.8.13) is $\frac{1}{16}\rho c\boldsymbol{u}\cdot\boldsymbol{u}$, i.e. the same $k'b$-order as (7.3)), but consider the cylinder entering still water with a steady and purely longitudinal velocity. The fluid kinetic energy is then constant, implying that the force must be zero.

The free-surface forces also have a transverse component, which can be written

$$\tfrac{1}{2}\tan\alpha\{-[\boldsymbol{t}\cdot(\boldsymbol{l}\wedge\boldsymbol{mu})]\,(\boldsymbol{l}\wedge\boldsymbol{u})+(\boldsymbol{t}\cdot\boldsymbol{u})\,\boldsymbol{mu}\} \tag{7.4}$$

by writing $\boldsymbol{t}$ for a transverse unit vector pointing out of the water in the plane of $\boldsymbol{l}$ and $\boldsymbol{n}$ (see figure 1), and $\boldsymbol{s} = \boldsymbol{l} \wedge \boldsymbol{t}$ for a transverse unit vector in the free surface, and noting that $\boldsymbol{l} \wedge \boldsymbol{u} = (\boldsymbol{t}\cdot\boldsymbol{u})\,\boldsymbol{s} - (\boldsymbol{s}\cdot\boldsymbol{u})\,\boldsymbol{t}$. The first term of (7.4) is exactly analogous to (7.2) and (7.3) in that it represents a three-dimensional potential-flow effect in principle

beyond current practice based on Morison's equation (7.1); but the second term is in a special category because for α near 90° current practice would be to make special provision for it as a 'slam load'. These slam loads are conventionally calculated (see e.g. Sarpkaya & Isaacson 1981, §5.5.2) on the basis of 'rate of change of momentum' which gives (since for a cylinder moving transversely the rate of change of wetted length is $\tan\alpha(\boldsymbol{t}\cdot\boldsymbol{u})$) the fluid force as $\tan\alpha(\boldsymbol{t}\cdot\boldsymbol{u})\,\boldsymbol{mu}$ which is exactly twice the second term of (7.4), and is completely spurious because that argument ignores the force on the far fluid boundary, which does not tend to zero with boundary distance (and if there is no far boundary then there is accordingly the famous classical conundrum that momentum is not defined, see Lamb 1932 §119)). Indeed, the work done against this slam load can be seen to be exactly twice the kinetic energy gain, whereas the work done against (7.4) (plus the work done against the submerged-end forces (7.2) and (7.3), which is non-zero if the cylinder velocity is not purely transverse) can be seen to be equal to the kinetic energy gain, as it should be. The force of this point is particularly evident in the case of a cylinder leaving the water surface rather than entering it: this time the spurious 'rate of change of momentum' argument leads to a force which does twice as much work as the kinetic energy loss!

In general, we saw in table 1 that steady-flow end effects do not vanish in our thin-cylinder (small-$k'b$) limit because the smallness of the areas involved (one $k'b$-order higher than the area of the cylinder sides) is offset by the bigness of the fluid velocities (one $k'b$-order lower than on the cylinder sides, given that the lowest-$k'b$-order side effects cancel via D'Alembert's paradox); it also follows that it is sufficient to use the lowest-$k'b$-order approximation to longitudinal and transverse fluid velocities when calculating steady-flow end effects. In particular, we can ignore the effects of longitudinal radiated/diffracted velocity (table 1, column 1 row 1) and incident velocity gradients (table 1, column 2), leading to the important conclusion that *the formulae* (7.2), (7.3) *and* (7.4) *for steady-flow end effects will be true in general if we replace* $\boldsymbol{u}$ *by the relative velocity* $(\boldsymbol{v}-\boldsymbol{u})$. This is in fact a searching test of the consistency of our equation of motion (6.8) – it can be shown for example (Rainey 1984) that (6.8) gives exactly the same forces, as it should, whether the (arbitrarily shaped) structure is moving into still water, or the water is moving (uniformly) onto a fixed structure. In the latter case it should of course be arranged that the surface pressure in the incident flow is strictly zero, or else the structure will feel an extra force pushing it through the wavy lid – this means, for example, that when a uniform current is considered it is necessary to lower the water level to compensate for the pressure drop from the last term in (2.6).

We have also seen in general that steady-flow end forces are proportional to velocity squared and thus of second $k'a'$-order, and proportional to cylinder cross-section and thus of second $k'b$-order (like all our thin-cylinder potential-flow forces, see §2). Morison's equation (7.1), by contrast, has its inertial term of first $k'a'$-order and second $k'b$-order, and its drag term of second $k'a'$-order and first $k'b$-order. The situation is summarized in table 2. Steady-flow end effects are thus comparable to the drag term rather than the inertia term in Morison's equation (in that they are proportional to velocity squared and thus of second order in $k'a'$), but are one order higher in $k'b$, and can thus be thought of as a 'higher $k'b$-order refinement of drag'. The criterion for their significance will therefore be based on the size of $k'b$ – and since they occur whenever cylinders have finite lengths, it will depend most generally just on the cylinder length aspect of k'. It can be established by considering the simplest case above, of a fully immersed circular cylinder in uniform translation. Setting $c_m = 2$ and $c_d = 1$ as agreed above, Morison's equation would predict a fluid load

		$k'b$-order	
		$k'b$	$(k'b)^2$
$k'a'$-order	$k'a'$		(i) Morison inertia term (ii) Unsteady-flow end effects
		(i) Morison drag term	(i) Steady-flow end effects
	$(k'a')^2$		(ii) Longitudinal diffracted/radiated flow effects (iii) Extensional incident flow effects

TABLE 2. $k'a'$-order and $k'b$-order of various fluid loads

on each half of the cylinder of ρblu_T^2 where $2l$ is the length of the cylinder, as against our end effects of $(\boldsymbol{u}\cdot\boldsymbol{l})\rho cu_T$. Evidently the significance of the end effects depends on $(\boldsymbol{u}\cdot\boldsymbol{l})/u_T$, i.e. the angle of the cylinder to the flow, which on an offshore structure typically varies during the wave cycle. It is reasonable to say in these circumstances that our end effects are significant if they are the largest fluid load for, say, 20% of the time, which sets our criterion at cylinder length/diameter < 10.

7.2. *Unsteady-flow end effects*

When we consider a fully immersed finite cylinder fixed in uniform but unsteady flow, we see from (6.8) that the potential-flow fluid loads are as for steady flow (i.e. the end effects (7.2) and (7.3), coming this time from the $\Delta e/\Delta X$ term in (6.8)) plus the load from the $-\mathrm{d}\boldsymbol{I}/\mathrm{d}t$ term in (6.8), which is (referring to (5.13)) in this case simply $\boldsymbol{m}'\dot{\boldsymbol{v}}$ per unit length. This additional load is exactly as would be predicted by the inertia term in Morison's equation, except that it includes a longitudinal force (from the ρc part of $\boldsymbol{m}'$) which is easily traceable to the incident-flow pressure difference across the cylinder ends. It is the now-familiar situation of the high $k'b$-order of the end area being counteracted by the low $k'b$-order of the pressures there, to give a result of comparable $k'b$-order to any other potential flow load. This time, however, the unsteady-flow end effects are exactly comparable with the inertia term in Morison's equation (being in fact of one half its maximum size if c_m is taken as 2 as agreed above), as shown in table 2, and will thus be significant whenever that term is important compared with the drag term. The criterion for this is well known to be that the amplitude of the water motion (typically the diameter of particle orbits in wave motion) is less than $5\times$ cylinder diameter, irrespective of the value of k'.

In the general case of a cylinder in waves intersecting the water surface, clearly only the immersed end will be affected, and indeed we see from (5.13) that the fluid load on a fixed cylinder is no longer simply $\boldsymbol{m}'\dot{\boldsymbol{v}}$ per unit length, but for example loses its longitudinal component, as it should do, if the immersed end is deep below the wave action (since ϕ_I is the integral of $\boldsymbol{v}$ along L).

7.3. *Longitudinal diffracted/radiated flow effects*

We noted in §2 that Lighthill (1979) found it necessary to include the effect of the longitudinal diffracted flow in his small-$k'b$ calculation of the wave loads on a vertical cylinder in waves. An example where this is the *only* (distributed) potential-flow load is a fully immersed weightless circular cylinder moving steadly in a circle in still water, always remaining symmetrically tangential to the circle, as illustrated in figure 2. Writing u for the longitudinal component of the cylinder's velocity, $2l$ for

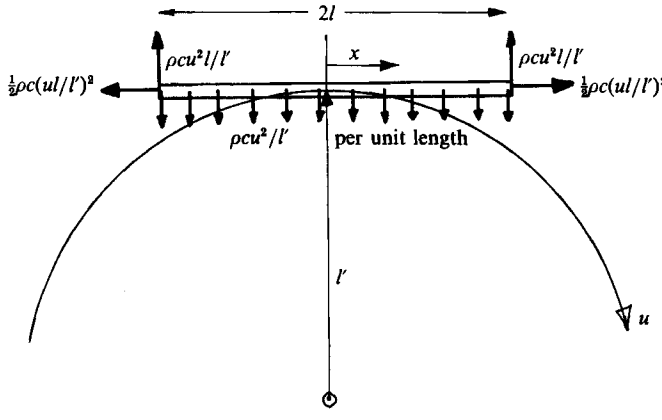

FIGURE 2. Fluid forces on a cylinder moving in a circle.

its length, and l' for the radius of the circle, we can write down the end forces on the cylinder as $\frac{1}{2}\rho c(ul/l')^2$ and $\rho cu^2l/l'$, as shown, using (7.2) and (7.3). Our equation (6.8) gives the total fluid load as zero (taking R as the centre of the cylinder, so that $\boldsymbol{m}$ is continuously zero and $\boldsymbol{h}$ is a constant), however, so we deduce that there must be a centripetal fluid load $2\rho cu^2l/l'$ disributed along the cylinder, as shown. This is the 'negative centrifugal force' of airship aerodynamics, where it was first explained (Munk 1936, figure 3) by a heuristic momentum argument, an argument which was later generalized and proved by direct pressure integration by Lighthill (1960). It is traceable to the effect of the longitudinal radiated flow: the radiated potential (see (2.4)) will appear constant to an observer rotating with the cylinder, so that the first pressure term in (2.6) is $\rho\boldsymbol{u}\cdot\nabla\phi$, whose effect cancels out by symmetry around the cylinder except for the contribution from the longitudinal flow, which is $\rho cu^2/l'$ per unit length. The effect of the second pressure term in (2.6) also cancels out by symmetry. In general we can see that these longitudinal-flow loads, like steady-flow end loads, will be of second order in both $k'a'$ and $k'b$, see table 2.

Morison's equation (7.1) will produce zero fluid load from the inertial term (unless u is understood as a vector, which would lead to the ridiculous conclusion that a torus rotating about its axis in still water would feel a centrifugal fluid load, since $\dot{u}$ would be centripetal), and a pure couple from the drag term. Taking $c_d = 1$ as agreed above, the local load from the drag term will be $\rho b(ux/l')^2$ at a distance x from the centre of the cylinder, which is greater than our potential-flow distributed load provided $(x/l')^2 > \pi(b/l')$. This is exactly as at the end of §7.1 above: when the incident angle of the cylinder to the flow is small the potential-flow dominates, when it is large the vorticity-flow load dominates. Taking the same angle of incidence as there as the threshold for practical significance, we conclude that these potential-flow loads become significant if the motion radius (to the instantaneous centre of rotation) is less than 20 times the cylinder diameter.

7.4. *Direct effects of incident velocity gradients*

The only case where the second-$k'a'$-order potential flow load is traceable *only* to the direct effect of $\boldsymbol{v}$ (i.e. the second term in (2.4)) is the two-dimensional problem of a fully immersed cylinder fixed parallel to the crests of the waves. This problem is also unique in that it can be readily studied using the result in Taylor (1928*b*) noted extensively above, because such a cylinder satisfies Taylor's requirement that *all* its

relevant dimensions are small compared with a wavelength. As apparently first pointed out by Isaacson (1979), Taylor's steady-flow calculation corresponds to the part of the general unsteady-flow loading coming from the second pressure term in (2.6), and moreover the surface integral of the first pressure term has simple small-$k'b$ limiting properties, so we can obtain the total potential-flow load on our cylinder as (Isaacson 1979, equation 17; since $\boldsymbol{v}$ is symmetric we can write Isaacson's components of $\boldsymbol{v}^{\mathrm{T}}$ as $\boldsymbol{v}$)

$$\boldsymbol{m}'\dot{\boldsymbol{v}}+\boldsymbol{v}\boldsymbol{m}'\boldsymbol{v} \tag{7.5}$$

per unit length, which agrees, as it should, with our equation (6.8). (Incidentally, Taylor's general result for a small body would be in our notation $\boldsymbol{v}\boldsymbol{m}'\boldsymbol{v}$ with $\boldsymbol{m}'$ representing the three-dimensional added mass and volume, see also Lighthill 1986*b*, equation 24, so for the general small-body case Isaacson should have obtained (7.5) with this meaning for $\boldsymbol{m}'$, which would also be given by (6.8). However, Isaacson's general small-body result (Isaacson 1979, equation 15 and Sarpkaya & Isaacson 1981, equation 5.5) is incorrect, containing an erroneous factor of a half in the off-diagonal parts of $\boldsymbol{v}$, traceable to Isaacson 1979, equation 6.)

The inertia term in Morison's equation only gives the first term in (7.5) (although when the cylinder is circular, we could obtain the correct answer by substituting the particle acceleration $\dot{\boldsymbol{v}}+\boldsymbol{v}\boldsymbol{v}$ for $\dot{\boldsymbol{v}}$, as pointed out by Isaacson (1979, equation 28)), which is correct to first $k'a'$-order. The second term in (7.5), coming from the incident velocity gradient, is of second $k'a'$-order, see table 2, and is thus of size exactly comparable with the drag term in Morison's equation (although of course generally acting in a different direction), with $c_d = \pi kb$ (since $\boldsymbol{v} \sim k\boldsymbol{v}$). Taking once more a circular cylinder and a drag term with $c_d = 1$ to find the criterion for practical significance, and taking the vertical forces for comparison (since $\boldsymbol{v}\boldsymbol{v}$ is typically vertical in this case, see below) we see that again the relative size of the two forces depends on the timing, with our 20% rule giving the criterion for the significance of direct effects of incident velocity gradients as wave length/cylinder diameter < 30.

In all other cases the direct effects of incident velocity gradients are combined with a longitudinal-flow effect like §7.3 above, so that Taylor's result no longer gives the potential-flow load per unit length on the cylinder, although Lighthill (1986*b*, §11) inexplicably implies that it does. The best illustration of this point is in fact the fixed vertical circular cylinder example in Lighthill (1979), which correctly includes the effects of longitudinal diffracted flow and gives the second-$k'a'$-order potential flow load as (Lighthill 1979, equation 43) the horizontal component of

$$-\boldsymbol{v}\boldsymbol{m}\boldsymbol{v} \tag{7.6}$$

per unit length, or, given that $\boldsymbol{v}\boldsymbol{v}$ is vertical and $\dot{\boldsymbol{v}}$ is purely first $k'a'$-order in Lighthill's example, *minus* Taylor's result (7.5). This agrees, as it should, with our general result (6.8), as may be seen most readily by considering a finite length of the cylinder and noting that the sum of the transverse forces (7.2) at the cylinder ends can be written

$$-\int_L \boldsymbol{l}\cdot\nabla\{(\boldsymbol{l}\cdot\boldsymbol{v})\,\boldsymbol{m}\boldsymbol{v}\} = -\int_L \{(\boldsymbol{l}\cdot\boldsymbol{v}\boldsymbol{l})\,\boldsymbol{m}\boldsymbol{v}+(\boldsymbol{l}\cdot\boldsymbol{v})\,\boldsymbol{m}\boldsymbol{v}\boldsymbol{l}\} = -\int_L \boldsymbol{m}\{\boldsymbol{l}\cdot\boldsymbol{v}\boldsymbol{l}(\boldsymbol{t}'\cdot\boldsymbol{v})+\boldsymbol{t}'\cdot\boldsymbol{v}\boldsymbol{l}(\boldsymbol{l}\cdot\boldsymbol{v})\}\,\boldsymbol{t}' \tag{7.7}$$

where $\boldsymbol{t}'$ is a unit vector perpendicular to the cylinder axis and wave crests. By Laplace's equation we can write $\boldsymbol{l}\cdot\boldsymbol{v}\boldsymbol{l}+\boldsymbol{t}'\cdot\boldsymbol{v}\boldsymbol{t}' = 0$ so this becomes

$$\int_L \boldsymbol{m}\boldsymbol{v}\{(\boldsymbol{t}'\cdot\boldsymbol{v})\,\boldsymbol{t}'-(\boldsymbol{l}\cdot\boldsymbol{v})\,\boldsymbol{l}\} = \int_L \boldsymbol{m}\boldsymbol{v}\{2(\boldsymbol{t}'\cdot\boldsymbol{v})\,\boldsymbol{t}'\} = 2\int_L (\boldsymbol{t}'\cdot\boldsymbol{v}\boldsymbol{m}\boldsymbol{v})\,\boldsymbol{t}' \tag{7.8}$$

using the fact that $\boldsymbol{vv}$ is vertical in the given waves (so that $\boldsymbol{mvv} = 0$), and finally the fact that in our case $\boldsymbol{m}$ is a scalar times $(\boldsymbol{t}')\boldsymbol{t}'\cdot$. Adding (7.6) and (7.8) gives a total equivalent horizontal force per unit length equal to the horizontal component of $\boldsymbol{vmv}$, which agrees with the prediction of (6.8) given again that $\boldsymbol{vv}$ is vertical. Lighthill's choice of second $k'a'$-order, deep water, and an infinite vertical cylinder in fact neatly avoids end effects as noted in §2, so we can alternatively show that if the free surface and infinite length is taken into account, the prediction of (6.8) reduces to (7.6) integrated along the whole cylinder, as it should. The algebra is longer though – the integral of the horizontal component (in the direction of wave travel) of (7.6) becomes to second $k'a'$-order

$$-\frac{1}{2}\frac{\rho c k^2}{\omega}\phi_1\dot{\phi}_1, \tag{7.9}$$

where ω is the wave angular frequency and $\phi_1, \dot{\phi}_1$ are evaluated at the surface intersection. The $\Delta e/\Delta X$ term in (6.8) then gives minus (7.9) from its line integral part and minus four times (7.9) from its surface intersection part, the $-\mathrm{d}\boldsymbol{I}/\mathrm{d}t$ term in (6.8) gives four times (7.9) from its surface intersection part and four times (7.9) from $\dot{L}$ in $\mathrm{d}/\mathrm{d}t$ (5.13), and finally the hydrostatic part of $\boldsymbol{Q}$ in (6.8) (i.e. (6.3)) gives minus two times (7.9), making in all (7.9) as required. Lighthill's additional 'waterline force' (Lighthill 1979, equation 34, and 1986*b*, equation 33) can be left out of the reckoning because it is equivalent to the effect from the varying length of L in the $\int_L \boldsymbol{m}'\dot{\boldsymbol{v}}$ term in $\mathrm{d}/\mathrm{d}t$ (5.13), and would also incidentally be included by the standard practice of applying Morison's equation up to the instantaneous level of the incident wave.

8. Conclusions

The potential-flow fluid loading on partially immersed lattice structure moving in waves is given, to second order in wave height, by

$$\frac{\mathrm{d}\boldsymbol{N}}{\mathrm{d}t} = \boldsymbol{Q} - \frac{\mathrm{d}\boldsymbol{I}}{\mathrm{d}t} + \{0, (\boldsymbol{m}+\boldsymbol{j}) \wedge \boldsymbol{v}\} + \frac{\Delta e}{\Delta X}, \tag{8.1}$$

where $\boldsymbol{N} = (\boldsymbol{m}, \boldsymbol{h})$ is the translational and angular 'momentum' of the structure based on its instantaneous added mass calculated in two-dimensional style as in Morison's equation. $\boldsymbol{Q}$ is the external force and moment on the structure from non-hydrodynamic sources, and the fluid loading terms are given by

$$\boldsymbol{I} = (\boldsymbol{j}, \boldsymbol{k}) = \left\{\left(-\int_L \boldsymbol{m}'\boldsymbol{v} + \rho\sum_p \phi_1 \boldsymbol{n}c/\cos\alpha\right), \left(-\int_L \boldsymbol{r}\boldsymbol{m}'\boldsymbol{v} + \rho\sum_p \phi_1 \boldsymbol{r}\boldsymbol{n}c/\cos\alpha\right)\right\}, \tag{8.2}$$

$$\frac{\Delta e}{\Delta X} = \int_L \{\boldsymbol{v}\boldsymbol{m}'(\boldsymbol{v}-\boldsymbol{u}), [\boldsymbol{r}\boldsymbol{v}\boldsymbol{m}'(\boldsymbol{v}-\boldsymbol{u}) - \boldsymbol{v} \wedge \boldsymbol{m}'(\boldsymbol{v}-\boldsymbol{u})]\} + \sum_p \boldsymbol{S}. \tag{8.3}$$

Since these are all line integrals along the lattice-member centrelines, plus simple summations over their intersections with the free surface, (8.1) can be solved computationally by a Morison-equation-type computer program.

The effects of vorticity can be included to the same order of accuracy by vortex momentum calculations (Lighthill 1986*b*), or approximately included by the drag term in Morison's equation. In the latter case the combined formulation is a worthwhile improvement on Morison's equation when any one of the conditions: (i) lattice member length/diameter < 10; or (ii) relative fluid motion/lattice member diameter < 5; or (iii) radius of structural motion/lattice member diameter < 20; or (iv) wavelength/lattice member diameter < 30; is satisfied.

The production of this paper has been basically a spare-time activity over a number of years, and owes a great deal to the continuing encouragement from my wife and family, and from the UK academic community. The original version (released to the Canadian library system as Rainey 1984) contains essentially all the above results, and was kindly sent to Sir James Lighthill by Professor J. M. T. Thompson. This led to the addition of a proof that the wavy-lid approximation is correct to second order in wave height – contrary to the claim in Rainey (1984) that it is exact. Further encouragement from Dr P. Sayer and Professor F. Ursell in 1986 led to a general simplification of the argument, with the relegation of the coordinate elimination to an Appendix, and a lengthier exposition of Lighthill (1979).

The UK Department of Energy began in 1986 to support the development of a computer program, based on this paper and the Atkins AQWA software, for use in the study of the capsize of semisubmersible oil rigs. This has latterly brought the work onto a full-time basis – the author particularly acknowledges the suggestion from Dr S. L. Smith to include an explicit calculation of $\Delta e/\Delta \boldsymbol{X}$. In contrast to the classical emphasis of much of the paper, Dr Smith had shown the relevance and power of computational methods by computer-debugging Appendix C, comparing $\Delta e/\Delta \boldsymbol{X}$ with $\delta e/\delta \boldsymbol{X}$ as described at the end of §6. Finally the author is grateful to Dr A. M. Mackey, Dr R. G. Standing, and one of the referees for drawing his attention to (respectively) the work of Munk (1936), Mavrakos (1988), and Havelock (1940), cited above.

Appendix A. Notation scheme

To keep the algebra manageable in this paper, it is necessary to adopt a special notation, in which single symbols denote scalars, 3- or 6-dimensional vectors, 3- or 6-dimensional linear mappings, or spatial features, depending on the typeface used. Standard practice is followed systematically for scalars, 3-dimensional vectors and spatial features: thus, for example, v is a scalar giving a velocity component in a particular axis system (see (2.3)), $\boldsymbol{v}$ is the vector describing the fluid velocity in the incident wave (see (5.3)), and V denotes the total volumetric extent of the water (see figure 1). Additional typefaces are then used systematically for 6-dimensional vectors, and 3- and 6-dimensional linear mappings. To aid readability, the symbols in these latter categories are listed below, in the order in which they appear, with the point of first occurrence given for each.

6-dimensional vectors

$\boldsymbol{U}$ structural velocity and angular velocity i.e. $\boldsymbol{U} = (\boldsymbol{v}, \boldsymbol{\omega})$ (5.11)
$\boldsymbol{I}$ 'wave impulse' (5.11), $= (\boldsymbol{j}, \boldsymbol{k})$ (6.2)
$\boldsymbol{N}$ structural 'impulse' $= \boldsymbol{M}^*\boldsymbol{U} = (\boldsymbol{m}, \boldsymbol{h})$ (6.2)
$\boldsymbol{Q}$ non-hydrodynamic force (acting at R) and moment (6.2)
$\boldsymbol{X}$ incremental position, i.e. $\delta \boldsymbol{X} = \boldsymbol{U}\delta t$ (A 2.2)
$\boldsymbol{P}_i$ generalized velocity vectors, i.e. $\boldsymbol{U} = \boldsymbol{P}_i \dot{q}_i$ (B 3)
$\boldsymbol{S}$ see (C 6)

3-dimensional linear mappings

$\boldsymbol{m}$ 2-dimensional added mass (per unit length) considered as a 3-dimensional mapping (5.9)
$\boldsymbol{m}'$ $\boldsymbol{m} + \rho c$ (5.12)
$\boldsymbol{r}$ $\boldsymbol{r} \wedge$ considered as a 3-dimensional mapping (5.13)
$\boldsymbol{v}$ velocity gradient mapping (6.9)

6-dimensional mappings

$\boldsymbol{M}$ 6-dimensional added mass (5.15)

$\boldsymbol{M^*}$ 6-dimensional mass (6.1)

Appendix B. Elimination of generalized coordinates

The generalized Lagrange coordinates q_i of (6.1) give an incremental change of any variable f as

$$\delta f = \frac{\partial f}{\partial t} + \frac{\partial f}{\partial q_i}\delta q_i + \frac{\partial f}{\partial \dot{q}_i}\delta \dot{q}_i. \tag{B 1}$$

We wish instead to use the general vector notation in which an incremental position change is written $\delta \boldsymbol{X} = \boldsymbol{U}\delta t$ and correspondingly an incremental variable change is written

$$\delta f = \frac{\partial f}{\partial t}\delta t + \frac{\partial f}{\partial \boldsymbol{X}}\cdot\delta \boldsymbol{X} + \frac{\partial f}{\partial \boldsymbol{U}}\cdot\delta \boldsymbol{U} \tag{B 2}$$

If we define unit generalized velocity 6-vectors by

$$\boldsymbol{U} = \boldsymbol{P}_i \dot{q}_i \tag{B 3}$$

then we can describe the non-hydrodynamic force (acting at R) and moment as a 6-vector $\boldsymbol{Q}$ and its rate of working as $\boldsymbol{Q}\cdot\boldsymbol{U}$, which means that by definition

$$f_i \dot{q}_i = \boldsymbol{Q}\cdot\boldsymbol{U} = \boldsymbol{Q}\cdot\boldsymbol{P}_i\dot{q}_i, \tag{B 4}$$

so that on the right-hand side of (6.1) $f_i = \boldsymbol{Q}\cdot\boldsymbol{P}_i$. Also, from (B 3) $\boldsymbol{P}_i\delta q_i = \boldsymbol{U}\delta t = \delta \boldsymbol{X}$ so for any variable which is independent of $\boldsymbol{U}$ we see from (B 1) and (B 2) that

$$\frac{\partial}{\partial q_i} = \boldsymbol{P}_i\cdot\frac{\partial}{\partial \boldsymbol{X}}. \tag{B 5}$$

Thus the second term on the left-hand side of (6.1) can be differentiated term-by-term and written (remembering that $\boldsymbol{M^*}$ is symmetric) as

$$-\frac{\partial \boldsymbol{U}}{\partial q_i}(\boldsymbol{I}+\boldsymbol{M^*U}) - \boldsymbol{P}_i\cdot\frac{\partial e_F}{\partial \boldsymbol{X}} - \left\{\left(\boldsymbol{P}_i\cdot\frac{\partial}{\partial \boldsymbol{X}}\right)\boldsymbol{I}\right\}\cdot\boldsymbol{U} - \tfrac{1}{2}\boldsymbol{U}\cdot\left\{\left(\boldsymbol{P}_i\cdot\frac{\partial}{\partial \boldsymbol{X}}\right)\boldsymbol{M^*}\right\}\boldsymbol{U}. \tag{B 6}$$

Because $\partial/\partial \boldsymbol{X}$ treats $\boldsymbol{U}$ as a constant this can be written

$$-\frac{\partial \boldsymbol{U}}{\partial q_i}(\boldsymbol{I}+\boldsymbol{M^*U}) - \boldsymbol{P}_i\cdot\frac{\partial}{\partial \boldsymbol{X}}(e_F + \boldsymbol{I}\cdot\boldsymbol{U} + \tfrac{1}{2}\boldsymbol{U}\cdot\boldsymbol{M^*U}). \tag{B 7}$$

The first term on the left-hand side of (6.1) can likewise be differentiated term-by-term and written, by virtue of (B 3):

$$\frac{\mathrm{d}}{\mathrm{d}t}\left\{\frac{\partial \boldsymbol{U}}{\partial \dot{q}_i}(\boldsymbol{I}+\boldsymbol{M^*U})\right\} = \frac{\mathrm{d}}{\mathrm{d}t}\{\boldsymbol{P}_i(\boldsymbol{I}+\boldsymbol{M^*U})\} = \dot{\boldsymbol{P}}_i(\boldsymbol{I}+\boldsymbol{M^*U}) + \boldsymbol{P}_i\cdot\frac{\mathrm{d}}{\mathrm{d}t}(\boldsymbol{I}+\boldsymbol{M^*U}). \tag{B 8}$$

All the terms of (6.1) apart from the first terms in (B 7) and (B 8) viz:

$$\left(\dot{\boldsymbol{P}}_i - \frac{\partial \boldsymbol{U}}{\partial q_i}\right)\cdot(\boldsymbol{I}+\boldsymbol{M^*U}), \tag{B 9}$$

have now been expressed as a scalar product with $\boldsymbol{P}_i$, which would mean, since $\boldsymbol{P}_i$ form a linearly independent set, that $\boldsymbol{P}_i$ could be eliminated to leave the required vector equation.

It is possible to express (B 9) as a scalar product with $\boldsymbol{P}_i$ by considering q_i to be the Cartesian coordinates of R for $i = 1,2,3$ and successive rotations about three arbitrary fixed axes for $i = 4,5,6$. The latter alone define the structure's angular velocity, so we can write

$$\boldsymbol{\omega} = \boldsymbol{P}_j \dot{q}_j = (\boldsymbol{0}, \boldsymbol{p}_j)\dot{q}_j, \tag{B 10}$$

where $j = 1,2,3$ corresponds to $i = 4,5,6$. Writing $\boldsymbol{M}^*\boldsymbol{U} = \boldsymbol{N} = (\boldsymbol{m}, \boldsymbol{h})$ and $\boldsymbol{I} = (\boldsymbol{j}, \boldsymbol{k})$, we can thus write (B 9) as

$$\left\{(\boldsymbol{0}, \dot{\boldsymbol{p}}_j) - \frac{\partial}{\partial q_i}(\boldsymbol{v}, \boldsymbol{\omega})\right\} \cdot \{(\boldsymbol{j}, \boldsymbol{k}) + (\boldsymbol{m}, \boldsymbol{h})\} = \left(\dot{\boldsymbol{p}}_j - \frac{\partial \boldsymbol{\omega}}{\partial q_j}\right) \cdot (\boldsymbol{k} + \boldsymbol{h}) = \left(\frac{\partial \boldsymbol{p}_j}{\partial q_k}\dot{q}_k - \frac{\partial \boldsymbol{p}_k}{\partial q_j}\dot{q}_k\right) \cdot (\boldsymbol{k} + \boldsymbol{h}). \tag{B 11}$$

Now since $q_j, j = 1,2,3$ are structural rotations in order about fixed axes, they will 'carry earlier $\boldsymbol{p}_j$ with them' so that

$$\frac{\partial \boldsymbol{p}_j}{\partial q_k} = 0 \quad \text{if} \quad j \geqslant k \quad \text{or} \quad \boldsymbol{p}_k \wedge \boldsymbol{p}_j \quad \text{if} \quad j < k. \tag{B 12}$$

Thus

$$\frac{\partial \boldsymbol{p}_j}{\partial q_k} - \frac{\partial \boldsymbol{p}_k}{\partial q_j} = \boldsymbol{p}_k \wedge \boldsymbol{p}_j. \tag{B 13}$$

So (B 11) becomes

$$(\boldsymbol{\omega} \wedge \boldsymbol{p}_j) \cdot (\boldsymbol{k} + \boldsymbol{h}) = \boldsymbol{p}_j \cdot \{(\boldsymbol{k} + \boldsymbol{h}) \wedge \boldsymbol{\omega}\} = \boldsymbol{P}_i \cdot \{\boldsymbol{0}, (\boldsymbol{k} + \boldsymbol{h}) \wedge \boldsymbol{\omega}\}, \tag{B 14}$$

which is the required scalar product with $\boldsymbol{P}_i$. The vector equation of motion of the structure is therefore

$$\frac{\mathrm{d}}{\mathrm{d}t}(\boldsymbol{I} + \boldsymbol{N}) + \{\boldsymbol{0}, (\boldsymbol{k} + \boldsymbol{h}) \wedge \boldsymbol{\omega}\} = \frac{\partial}{\partial \boldsymbol{X}}(e_{\mathrm{F}} + \boldsymbol{I} \cdot \boldsymbol{U} + \tfrac{1}{2}\boldsymbol{U} \cdot \boldsymbol{M}^*\boldsymbol{U}) + \boldsymbol{Q}. \tag{B 15}$$

Appendix C. The thin-cylinder expression for $\Delta e/\Delta \boldsymbol{X}$

Using (5.6)–(5.9) we can first write e as

$$e = e_{\mathrm{I}} + \frac{1}{2}\int_L (\boldsymbol{v} - \boldsymbol{u}) \cdot \boldsymbol{m}'(\boldsymbol{v} - \boldsymbol{u}) - \frac{1}{2}\int_L \rho c \boldsymbol{u} \cdot \boldsymbol{u} - \rho \sum_p \phi_{\mathrm{I}} (\boldsymbol{v} - \boldsymbol{u}) \cdot \boldsymbol{n} c / \cos\alpha. \tag{C 1}$$

$\Delta e/\Delta \boldsymbol{X}$ can most easily be evaluated by taking the viewpoint of an observer moving with the structure, to whom $\boldsymbol{U}$ and $\boldsymbol{m}'$ will appear fixed during the position increment $\delta \boldsymbol{X} = (\delta \boldsymbol{x}_1, \delta \boldsymbol{x}_2)$ used to define $\Delta/\Delta \boldsymbol{X}$ in (6.4)–(6.6), but $\boldsymbol{v}$ will, at any point on the structure, appear to change by

$$\delta \boldsymbol{v} = \boldsymbol{v}(\delta \boldsymbol{x}_1 + \delta \boldsymbol{x}_2 \wedge \boldsymbol{r}) + \boldsymbol{v} \wedge \delta \boldsymbol{x}_2. \tag{C 2}$$

If the structure is fully immersed, only the second term in (C 1) will appear to change, by an amount given (remembering that $\boldsymbol{m}'$ is symmetric) by

$$\int_L \{\boldsymbol{v}(\delta \boldsymbol{x}_1 + \delta \boldsymbol{x}_2 \wedge \boldsymbol{r}) + \boldsymbol{v} \wedge \delta \boldsymbol{x}_2\} \cdot \boldsymbol{m}'(\boldsymbol{v} - \boldsymbol{u}). \tag{C 3}$$

Writing $\boldsymbol{r}$ for $\boldsymbol{r} \wedge$, as in §5, and noting that $(\boldsymbol{vr})^{\mathrm{T}} = -\boldsymbol{rv}$ because $\boldsymbol{r}$ is skew-symmetric and $\boldsymbol{v}$ is symmetric, this can be rearranged as

$$\int_L [\boldsymbol{vm}'(\boldsymbol{v} - \boldsymbol{u}), \{\boldsymbol{rvm}'(\boldsymbol{v} - \boldsymbol{u}) - \boldsymbol{v} \wedge \boldsymbol{m}'(\boldsymbol{v} - \boldsymbol{u})\}] \cdot \delta \boldsymbol{X}. \tag{C 4}$$

If the structure is not fully immersed, there will in addition be changes to the integrals in (C 1) resulting from changes in the cylinders' wetted lengths. Now a cylinder motion parallel to the water surface does not change its wetted length, and a unit motion normal to the water surface gives a wetted length reduction of $(\cos\alpha)^{-1}$. The overall wetted length reduction is therefore the scalar product of $\boldsymbol{n}/\cos\alpha$ with cylinder motion, enabling the increment in (C 1) to be written

$$-\sum_p \frac{\frac{1}{2}[(\boldsymbol{v}-\boldsymbol{u})\cdot\boldsymbol{m}'(\boldsymbol{v}-\boldsymbol{u})-\rho c\boldsymbol{u}\cdot\boldsymbol{u}]\boldsymbol{n}}{\cos\alpha}\cdot(\delta\boldsymbol{x}_1+\delta\boldsymbol{x}_2\wedge\boldsymbol{r})$$

$$=-\sum_p \frac{\frac{1}{2}[(\boldsymbol{v}-\boldsymbol{u})\cdot\boldsymbol{m}'(\boldsymbol{v}-\boldsymbol{u})-\rho c\boldsymbol{u}\cdot\boldsymbol{u}](\boldsymbol{n},\boldsymbol{r}\wedge\boldsymbol{n})\cdot\delta\boldsymbol{X}}{\cos\alpha}. \quad \text{(C 5)}$$

Finally, we must for a partially immersed structure consider the last term in (C 1), which is only zero if the water is still. (The first term e_{I} in (C 1) can of course always be ignored, because it is in all respects independent of the structure, and thus never makes any contribution to $\Delta e/\Delta\boldsymbol{X}$.) The variation with our position increment of each constituent of this last term produces in each case an expression of comparable complexity to (C 5); these are however not reproduced here† because they are not required for any of the formulae in §7 above. Instead, we simply write the complete expression for $\Delta e/\Delta\boldsymbol{X}$ as

$$\int_L [\boldsymbol{v}\boldsymbol{m}'(\boldsymbol{v}-\boldsymbol{u}),\{\boldsymbol{r}\boldsymbol{v}\boldsymbol{m}'(\boldsymbol{v}-\boldsymbol{u})-\boldsymbol{v}\wedge\boldsymbol{m}'(\boldsymbol{v}-\boldsymbol{u})\}]+\sum_p \boldsymbol{S} \quad \text{(C 6)}$$

where the 6-dimensional vector $\boldsymbol{S}$ is the sum of the 6-dimensional vectors (in scalar product with $\delta\boldsymbol{X}$) in these expressions and (C 5).

REFERENCES

Angwin, J. 1986 Results of a joint semisubmersible/submersible wave drift force project. *Proc. Intl Symp. on Developments in Deeper Waters*, vol. 1, paper 12. London: Royal Institution of Naval Architects.

Batchelor, G. K. 1967 *An Introduction to Fluid Dynamics*. Cambridge University Press.

Eatock-Taylor, R. & Hung, S. M. 1985 Wave drift enhancement effects in multi-column structures. *Appl. Ocean Res.* **7**, 128–137.

Eatock-Taylor, R. & Jefferys, E. R. 1986 Variability of hydrodynamic load predictions for a tension leg platform. *Ocean Engng* **13**, 449–490.

Havelock, T. H. 1940 The pressure of water waves upon a fixed obstacle. *Proc. R. Soc. Lond.* A **175**, 409–421.

Isaacson, M. de St. Q. 1979 Nonlinear inertia forces on bodies. *J. Waterway Port, Coastal Ocean Div. ASCE* **105** (WW3), 213–227.

Isaacson, M. de St. Q. 1982 Nonlinear-wave effects on fixed and floating bodies. *J. Fluid Mech.* **120**, 267–281.

John, F. 1950 On the motion of floating bodies, II: Simple harmonic motions. *Comm. Pure Appl. Maths* **3**, 45–101.

Korsmeyer, F. T., Lee, C.-H. Newman, J. N. & Sclavounos, P. D. 1988 The analysis of wave effects on tension leg platforms. *Proc. OMAE Conf., Houston*, paper 88-611. New York: Soc. Naval Arch. & Mar. Eng.

Lamb, H. 1932 *Hydrodynamics*, 6th edn. Cambridge University Press.

Lighthill, M. J. 1960 Note on the swimming of slender fish. *J. Fluid Mech.* **9**, 305–317.

Lighthill, M. J. 1979 Waves and hydrodynamic loading. *Proc. 2nd Intl Conf. on the Behaviour of Offshore Structures*, vol. 1, pp. 1–40. Cranfield: BHRA Fluid Engineering.

† The complete expressions, with their derivation, are available from the *JFM* editorial office.

LIGHTHILL, M. J. 1986*a* *An Informal Introduction to Theoretical Fluid Mechanics*. Clarendon.

LIGHTHILL, M. J. 1986*b* Fundamentals concerning wave loading on offshore structures. *J. Fluid Mech.* **173**, 667–681.

LONGUET-HIGGINS, M. S. & COKELET, E. D. 1976 The deformation of steep surface waves on water, I: A numerical method. *Proc. R. Soc. Lond.* A **350**, 1–26.

MACCAMY, R. C. & FUCHS, R. A. 1954 Wave forces on piles: a diffraction theory. *Tech. Memo.* 69. Washington: US Army Corps of Engineers Beach Erosion Board.

MCIVER, P. 1987 Mean drift forces on arrays of bodies due to incident long waves. *J. Fluid Mech.* **185**, 469–482.

MAVRAKOS, S. A. 1988 The vertical drift force and pitch moment on axisymmetric bodies in regular waves. *Appl. Ocean Res.* **10**, 207–218.

MILNE-THOMSON, L. M. 1968 *Theoretical Hydrodynamics*, 5th edn. Macmillan.

MILOH, T. 1984 Hamilton's principle, Lagrange's method, and ship motion theory. *J. Ship Res.* **28**, 229–237.

MUNK, M. M. 1936 *Aerodynamics of Airships*, div. Q. In *Aerodynamic Theory* vol. VI, (ed. W. F. Durand). Springer.

NEW, A. L., MCIVER, P. & PEREGRINE, D. H. 1985 Computations of overturning waves. *J. Fluid Mech.* **150**, 233–251.

PEREGRINE, D. H., COKELET, E. D. & MCIVER, P. 1980 The fluid mechanisms of waves approaching breaking. *Proc. 17th Conf. Coastal Engng*, pp. 512–528. ASCE.

PINKSTER, J. A. 1979 Mean and low frequency wave drifting forces on floating structures. *Ocean Engng* **6**, 593–615.

RAINEY, R. C. T. 1984 *A New Equation for Calculating Wave Loads on Offshore Structures*. Montreal: Transport Canada Library, ref. 83186214 QC 157 R26.

RAINEY, R. C. T. 1986 A new theory and its application for stability criteria covering wave-induced tilt phenomena on semi-submersibles. *Proc. Intl Conf. Stationing and Stability of Semisubmersibles*, pp. 41–59. London: Graham & Trotman.

SARPKAYA, T. & ISAACSON, M. DE ST. Q. 1981 *Mechanics of Wave Forces on Offshore Structures*. Van Nostrand Reinhold.

STANDING, R. G., DACUNHA, N. M. C. & MATTEN, R. B. 1981 Mean wave drift forces: theory and experiment. *Rep.* OT-R-8175. London: Department of Energy.

TAYLOR, G. I. 1928*a* The energy of a body moving in an infinite fluid, with an application to airships. *Proc. R. Soc. Lond.* A **120**, 13–21.

TAYLOR, G. I. 1928*b* The forces on a body placed in a curved or converging stream of fluid. *Proc. R. Soc. Lond.* A **120**, 260–283.

THOMPSON, J. M. T. & STEWART, H. B. 1986 *Non Linear Dynamics and Chaos*. Wiley.

VINJE, T. & BREVIG, P. 1981 Numerical calculations of forces from breaking waves. *Proc. Intl Symp. on Hydrodynamics in Ocean Engng*, pp. 547–566. Trondheim: Norwegian Hydrodyn. Labs.

WEHAUSEN, J. V. & LAITONE, E. V. 1960 *Surface Waves*. In *Handbuch der Physik*, vol. 9, pp. 446–778. Springer.